The solid state and solution structures of tin(IV) alkoxide compounds and their use as precursors to form tin oxide ceramics via sol–gel-type hydrolysis and condensation

Mark J. Hampden-Smith[1], Teresa A. Wark

Department of Chemistry and Center for Micro-Engineered Ceramics, University of New Mexico, Albuquerque, NM 87131 (U.S.A.)

C. Jeffrey Brinker[2]

Sandia National Laboratories, P.O. Box 5800, Albuquerque, NM 87185 (U.S.A.)

CONTENTS

ABBREVIATIONS

acac	acetylacetonate
bzac	benzoylacetonate
COD	1,5-cyclooctadiene
pvm	dipivaloylmethane
OEt	ethoxide
O-i-Pr	i-propoxide
O-*n*-Bu	*n*-butoxide
O-*n*-Am	*n*-pentoxide
O-*t*-Am	*t*-pentoxide
ONp	neo-pentoxide
O-*n*-hexyl	*n*-hexoxide
O-Ph	phenoxide

---

[1]To whom correspondence should be addressed.
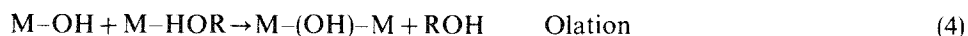[2]Currently adjunct Professor of Chemistry and Chemical Engineering, UNM.

O-*n*-hept	*n*-heptoxide
O-*n*-Oct	*n*-octoxide
OMe	methoxide
O-*n*-Pr	*n*-propoxide
O-CHEt$_2$	i-amyloxide
O-*t*-Bu	i-butoxide
O-i-Am	i-pentoxide
O-CHMe-*n*-Pr	2-pentoxide
O-CHMe-*n*-Bu	2-hexoxide
O-CEt$_3$	*t*-heptoxide
O-cyclohexyl	cyclohexoxide
O-CHEt-*n*-Bu	2-heptoxide

A. INTRODUCTION

The chemistry of metal alkoxide compounds was extensively studied in the 1960s and 1970s, notably by the groups of Bradley and Mehrotra [1]. Since that time, the interest in metal alkoxide chemistry has generally been focused on alkoxide ligand-supported metal complexes in which the alkoxide ligands are generally spectators to the central chemistry [2,3], with a few notable exceptions [4].

More recently, a resurgence in the interest of metal alkoxide chemistry has come about, mainly because these species can be used as precursors for the formation of metal oxides [5–11]. In particular, the hydrolysis and condensation of metal-organic compounds to form metal oxides via the so-called "sol–gel" process has received a great deal of attention, but many other processing techniques such as chemical vapor deposition (CVD) [12], spray pyrolysis [13], and aerosol methods [14] have also been used. The physical and chemical requirements of the metal alkoxide precursor for sol–gel-type hydrolysis and condensation are solubility, generally in alcohol solvents, and susceptibility to hydrolysis, often acid or base catalyzed.

The most common sol–gel process for preparing ceramics is based on the hydrolysis and condensation of metal alkoxide compounds [15]. Hydrolysis replaces the alkoxide groups with hydroxyl groups. Subsequent condensation reactions involving the hydroxyl groups produce M–O–M or M(μ-OH)M bonds in addition to other by-products such as water or ethanol [11].

$$M-OR + H_2O \rightarrow M-OH + ROH \qquad \text{Hydrolysis} \qquad (1)$$

$$M-OH + M-OR \rightarrow M-O-M + ROH \qquad \text{Alkoxolation} \qquad (2)$$

$$M-OH + M-OH \rightarrow M-O-M + H_2O \qquad \text{Oxolation condensation} \qquad (3)$$

$$M-OH + M-HOR \rightarrow M-(OH)-M + ROH \qquad \text{Olation} \qquad (4)$$

In this manner, inorganic polymers are constructed progressively, resulting ultimately (often after heating) in metal oxides. The advantages of sol–gel processing over conventional ceramic processing methods include the ability to make special shapes derived from the sol or the gel state (such as monoliths, films, fibers, and monosized powders) combined with compositional and microstructural control and low processing temperatures (see Fig. 1).

Silicates are, by far, the most widely studied sol–gel system [15]. By combining ^{1}H and ^{29}Si NMR spectroscopic investigations with small-angle scattering studies employing X-rays, neutrons or light, growth processes under different conditions of pH, solvent and water/Si molar ratio have been rationalized. Two types of kinetic growth processes are generally recognized (but not universally accepted): monomer–cluster growth and cluster–cluster growth [16,17]. Each of these processes may proceed under reaction-limited or diffusion-limited conditions. Monomer–cluster growth occurs exclusively by the addition of monomers to a growing polymer or particle called a cluster. Cluster–cluster growth occurs by the addition of monomers or clusters to other monomers or clusters. Once monomers are consumed, growth proceeds exclusively by the addition of clusters to clusters.

Control of structure at the molecular level has been demonstrated primarily for silicates where connections have been made between molecular structure (characterized by NMR spectroscopy, SAXS, vibrational spectroscopy, etc.) and microstructure (e.g. pore size, surface area, and sintering characteristics) [16–19]. These
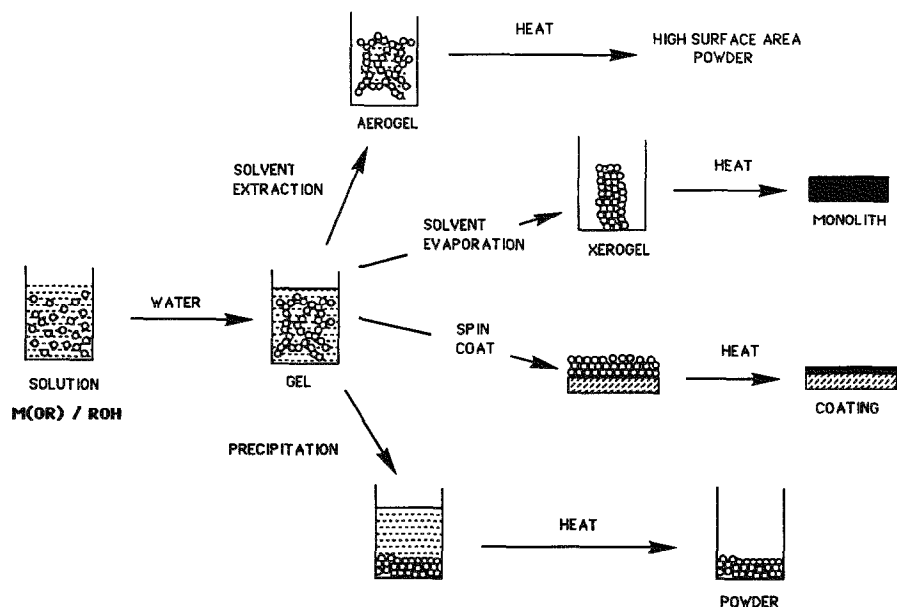

Fig. 1. Schematic diagram showing the versatility of the sol–gel processing technique for the formation of SiO_2 from silicon oxide compounds.

connections are more tenuous for non-silicate systems for the following reasons: (i) Most of the metals of interest to the ceramist (Ti, Zr, Sn, Al) are generally more electropositive than Si [1]. This causes the rates of hydrolysis and condensation to be orders of magnitude higher than for silicon with the result that hydroxide or oxohydroxide species precipitate immediately upon hydrolysis, unless special precautions are taken. (ii) Due to the rapidity of the hydrolysis and condensation processes, intermediates are difficult to isolate and characterize, so elucidation of the polymerization mechanisms is difficult. Under these conditions, it is difficult to isolate intermediate polymeric species necessary for microstructural control. (iii) The greater heat of formation of some metal oxides other than silicon provide a greater thermodynamic driving force to produce compact crystalline oxides rather than open polymeric species [20]. (iv) The greater lability of the M–O–M bonds contained in weakly branched polymers promotes restructuring to form highly condensed products.

Despite the apparent disadvantages of non-silicates, there are several factors that make non-silicates potentially more attractive from the standpoint of microstructural control. (i) Whereas silicon alkoxides are monomeric, more electropositive metal alkoxides are often oligomeric where the extent of oligomerization depends on the size of the metal and the steric demands of the alkoxide ligand substituents [1]. With appropriate chemical modification, these well-defined oligomers could be used as molecular building blocks. (ii) Silicon alkoxides have a preferred coordination number of four. Other metal alkoxides exhibit coordination numbers in the range 2–8, allowing a wide range of polymeric structures to be adopted. (iii) The d-orbital configuration of transition metal alkoxide compounds may be used to control structural diversity through ligand field stabilization [21].

Currently, the connections between polymer structure and microstructure in non-silicates are considerably tenuous. Based on kinetic growth processes, it is expected that the greater condensation rates of non-silicates establish diffusion-limited conditions, but this has not been well-documented to date, suggesting perhaps that restructuring (to form compact structures) occurs with kinetics commensurate to condensation. For example, monosized particles of pure or doped TiO_2, ZrO_2, and ZrO_2–Al_2O_3 have been prepared by the hydrolysis of homoleptic metal alkoxide precursors [22–27], while zinc oxide particles have been prepared by hydrolysis of ethyl-zinc tertiary butoxide [28]. We have recently demonstrated that tin(IV) ethoxide can be hydrolyzed under basic conditions to form spherical tin oxide particles with sizes in the range 70–250 nm, depending on the conditions [29]. These particles are composed of 2.0–3.0 nm crystallites of SnO_2 (cassiterite) which apparently have undergone an ordered aggregation process. This hierarchical structure is apparent in many non-silicate particles.

Livage et al. [11] have made the most important contributions to the understanding of hydrolysis and condensation of transition metal alkoxide compounds. They have attempted to rationalize the homogeneous growth of ceramic powders by consideration of the relative rates of hydrolysis and condensation, which they control

by various synthetic approaches. They emphasize that oligomerization, alcohol inter-change, acid/base catalysis, or complexation may be used to slow down hydrolysis and separate nucleation and growth steps in order to achieve monosized powders. For example, titanium alkoxide compounds containing primary alkoxide groups are thought to form trimers in alcohol solution with five-coordinate titanium centers, while those with secondary or tertiary alkoxide ligands remain monomeric due to the greater steric demands of the ligands [30,31]. Monomeric titanium alkoxide compounds such as $Ti(O-i-Pr)_4$ are thought to undergo hydrolysis and condensation simultaneously, leading to polydispersed powders while, under similar conditions, oligomeric titanium alkoxide compounds such as $Ti(OEt)_4$ form monosized spherical particles.

In order to derive the potential benefits of non-silicates without incurring their disadvantages, it is often necessary to modify the metal alkoxide precursors chemi-cally in order to reduce the overall hydrolysis and condensation rates and to reduce (temporarily) the effective functionality as a method of controlling the dimensionality and growth processes. This topic has been explored by Livage et al. [11,31–35]. Thus, whereas hydrolysis of $Ti(O-i-Pr)_4$ leads to formation of polydispersed 10–20 nm particles, hydrolysis of $[Ti(O-i-Pr)_3(acac)]$ results in formation of a colloidal sol consisting of ~ 5–10 nm particles, and hydrolysis of $(acac)_2Ti(O-i-Pr)_2$ results in formation of weakly branched polymers that may be useful precursors for formation of fibers [15,34,36].

While many studies of the hydrolysis and condensation of metal alkoxide compounds have been carried out, in general the solution structures of metal alkoxide compounds have not been extensively investigated, and relatively little is known about mechanistic aspects of hydrolysis and condensation. The connection between polymer structure and properties such as surface area, pore size, and pore volume of the final product have not been decisively made. These properties are of the utmost importance in the areas of membranes, catalysts, sensors, adsorbents, optical films, and acoustic or thermal insulators.

The alkoxide chemistry of the elements comprising the perovskite phase metal oxide superconductors, dielectrics, and ferroelectric ceramics are receiving particular attention [11]. Thus far, there has been little recent development in tin(IV) alkoxide chemistry since the work of Bradley et al. [37] and Marie [38], despite the fact that tin(IV) oxide and doped tin(IV) oxide exhibit a variety of interesting physical and chemical properties, most notably optical transparency and electrical conductivity [39]. These properties have led to applications such as transparent electrodes in opto-electronic devices, heat mirrors, thin film resistors, gas sensors, and wear-resistant coatings. The development of tin(IV) alkoxide chemistry may offer opportu-nities in the development of higher-purity tin(IV) oxide or doped tin(IV) oxide films or powders, control over surface area, porosity or pore volume. In addition, insight gained in a fundamental understanding of the mechanistic aspects of tin(IV) oxide formation may be applicable to other metal oxide systems. This therefore seems an

opportune time to review the chemistry of tin(IV) alkoxide compounds and the research carried out to date on the formation of tin(IV) oxide from these species.

B. SYNTHESIS AND CHARACTERIZATION OF TIN(IV) ALKOXIDE COMPOUNDS

(i) Synthetic routes

Tin(IV) alkoxides have been prepared by a variety of different methods common to many other metal alkoxide compounds. However, in some cases, these routes did not result in formation of the desired product or the products were not easily separated from other reaction products.

Reaction of tin(IV) chloride with an excess of alcohol does not lead to replacement of all the chloride ligands but to formation of mixed chloro-alkoxide species [38]. This is a common feature of this reaction method. In the presence of a base such as ammonia, Marie has claimed that pure homoleptic tin(IV) alkoxide compounds can be prepared [38]. This has been disputed by Bradley et al. who found that reaction of tin(IV) chloride with alcohols in the presence of ammonia always resulted in contamination of the product with chloride- and nitrogen-containing impurities that could not be separated [37].

Salt-elimination reactions resulted in the formation of a double alkoxide according to the equation [37]

$$2SnCl_4 + 9NaOEt \rightarrow NaSn_2(OEt)_9 + 8NaCl \tag{5}$$
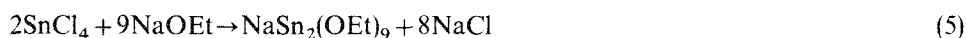
On further treatment with hydrogen chloride, tin(IV) ethoxide could be liberated as shown by

$$NaSn_2(OEt)_9 + HCl \rightarrow 2Sn(OEt)_4 + NaCl + EtOH \tag{6}$$
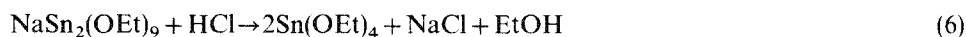
The reaction of lithium aryloxides, such as 2,6-diphenylphenoxide, with $SnCl_4$ results in the formation of cyclometallated products [40,41].

$$SnCl_4 + 2LiOAr \rightarrow 0.5[Cl_2Sn(OC_6H_3PhC_6H_4)]_2 + HOAr + 2LiCl \tag{7}$$
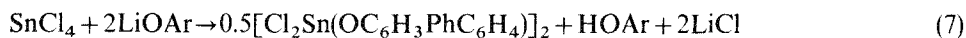
A better method seems to be the base-catalyzed alcoholysis of $SnCl_4$ using diethylamine as the base [42–44]. Slow addition of two equivalents of diethylamine to $SnCl_4$ resulted in an extremely exothermic reaction to form the corresponding bis-Lewis base adduct according to the equation

$$SnCl_4 + 2NHEt_2 \rightarrow SnCl_4(HNEt_2)_2 \tag{8}$$

Once two equivalents of diethylamine have been added, two more can be added rapidly with no further reaction. The subsequent addition of alcohol resulted in the

formation of the desired tin(IV) alkoxide compound together with formation of four equivalents of diethylammonium chloride.

$$SnCl_4(HNEt_2)_2 + 2HNEt_2 + 4HOR \rightarrow Sn(OR)_4 + 4H_2NEt_2 + Cl^- \qquad (9)$$

The separation of the tin(IV) alkoxide compound is easiest if it is soluble in non-polar organic solvents or, as in $Sn(O-t-Bu)_4$, is volatile and can be separated and isolated by sublimation. For $Sn(O-t-Bu)_4$, this method results in relatively high yields of approximately 80%. This method was patented by Thomas in 1976 [44].

The use of pyridine in the place of diethylamine in this reaction results in the formation of the bis(pyridine) adduct, $SnCl_4(py)_2$, which is not susceptible to alco-holysis with isopropanol [37].

$$SnCl_4 + 2py + HO-i-Pr \rightarrow SnCl_4(py)_2 + 4HO-i-Pr \qquad (10)$$
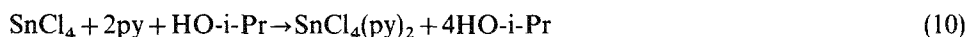
As an alternative, tin(IV) amides such as $Sn(NMe_2)_4$ can be treated with an excess of alcohol to liberate dimethylamine that is generally easily removed, resulting in formation of pure material [45].

$$Sn(NMe_2)_4 + 4HOR \rightarrow Sn(OR)_4 + 4HNMe_2 \qquad (11)$$
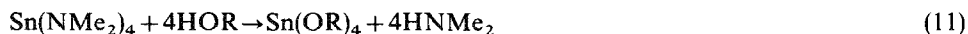
Where the alkoxide ligand is sterically demanding, it has been possible to isolate mixed amide alkoxide species. Thus, addition of two equivalents of 4-methyl-2,6-di-tert-butylphenol to $Sn(NMe_2)_4$ resulted in the isolation of $Sn(OAr)_2(NMe_2)_2$ [40].

$$Sn(NMe_2)_4 + 2HOAr \rightarrow Sn(OAr)_2(NMe_2) + 2HNMe_2 \qquad (12)$$
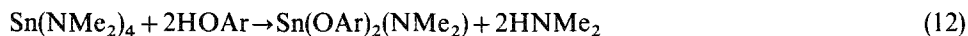
The product was structurally characterized in the solid state by single-crystal X-ray diffraction and found to be monomeric. On the other hand, the addition of two equivalents of 2,6-diphenylphenol to $Sn(NMe_2)_4$ resulted in formation of a cyclo-metallated product [35].

In cases where the alkoxide ligand has low steric demands, the liberated dimethylam-ine may coordinate to the metal center and prevent extensive oligomerization. This was recently observed for the case of benzyl alcohol [46].

$$Sn(NMe_2)_4 + 4HOBz \rightarrow 0.5Sn_2(OBz)_8(HNMe_2)_2 + 2HNMe_2 \qquad (14)$$

Such retention of liberated amine in the metal coordination sphere has been fre-quently observed in other metal alkoxide systems [47].

The final method of preparation of tin(IV) alkoxide compounds, used extensively, is trans alcoholysis.

$$Sn(OR)_4 + 4HOR' \rightarrow Sn(OR')_4 + 4HOR \tag{15}$$

This reaction is particularly facile if the pK_a of the alcohol added is lower than that of the alcohol being liberated. However, thermodynamically unfavorable products can be prepared by driving the reaction to the right through removal of the liberated alcohol, typically by azeotropic distillation with benzene [48].

Mixed tin(IV) alkoxides, $Sn(O\text{-}t\text{-}Bu)_{4-x}(OR')_x$, have been prepared by Mehrotra and Gupta [49] by stoichiometric reaction of $Sn(O\text{-}t\text{-}Bu)_4$ with different primary alcohols.
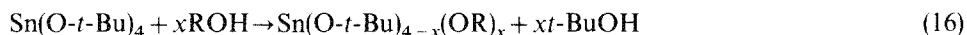
$$Sn(O\text{-}t\text{-}Bu)_4 + xROH \rightarrow Sn(O\text{-}t\text{-}Bu)_{4-x}(OR)_x + xt\text{-}BuOH \tag{16}$$

However, the species $Sn(O\text{-}t\text{-}Bu)_3(OR)$ and $Sn(O\text{-}t\text{-}Bu)_2(OR)_2$ undergo ligand redistribution according to the equation
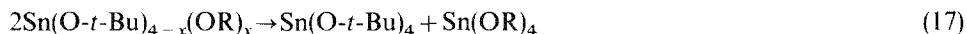
$$2Sn(O\text{-}t\text{-}Bu)_{4-x}(OR)_x \rightarrow Sn(O\text{-}t\text{-}Bu)_4 + Sn(OR)_4 \tag{17}$$

(ii) Characterization

(a) Physical properties

Homoleptic tin(IV) alkoxide compounds have been characterized by a variety of spectroscopic techniques to elucidate their structure and by a variety of physical methods to determine their molecular complexity. The range of homoleptic tin(IV) alkoxide compounds that have been prepared, their physical properties, and molecular complexities are given in Table 1. It is noteworthy that the molecular complexities determined in solution may have been measured under different conditions and therefore may not be strictly comparable. There are also some contradictory data in the literature, especially concerning whether or not certain derivatives can be recovered unchanged after distillation.

It also seems that some of the homoleptic tin(IV) alkoxide compounds exist as red-yellow liquids. As expected from the results for other metal alkoxide systems, as the steric demands of the alkoxide ligands increase, the degree of molecular complexity decreases and the volatility generally increases. For example, tin(IV) ethoxide is a tetramer, tin(IV) isopropoxide is a trimer, and tin(IV) tertiary butoxide is monomeric as determined cryoscopically by freezing point depression of benzene and ebullioscopically in boiling benzene. The presence of Lewis bases can alter the degree of aggregation by competing with alkoxide ligand lone pairs for vacant Lewis acidic sites at the tin center. This is exemplified in the case of tin(IV) isopropoxide which is trimeric in the absence of isopropanol, but forms a 1:1 adduct in the presence of the alcohol, $[Sn(O\text{-}i\text{-}Pr)_4 \cdot HO\text{-}i\text{-}Pr]_2$, which is dinuclear both in the solid state and in solution [42].

TABLE 1

Physical properties of homoleptic tin(IV) complexes

Empirical formula	Molecular complexity	Physical properties	Ref.
$Sn(OMe)_4$	4.1	Solid	38
	"Highly associated"	Solid	49
		B.P. 230°C/5 mm	
$Sn(OEt)_4$	4.0	Solid	38
$Sn(O\text{-}n\text{-}Pr)_4$	3.85	Solid	38
$Sn(O\text{-}i\text{-}Pr)_4$	3.10	Solid	38
		B.P. 131°C/1.6 mm	1
$Sn(O\text{-}n\text{-}Bu)_4$	3.70	Solid	38
$Sn(O\text{-}n\text{-}Am)_4$	1.5	Yellow liquid	38
$Sn(O\text{-}i\text{-}Am)_4$	1.05	Yellow liquid	38
$Sn(O\text{-}CHMe\text{-}n\text{-}Pr)_4$	1.15	Yellow liquid	38
$Sn(O\text{-}CHEt_2)_4$	1.15	Yellow liquid	38
$Sn(O\text{-}t\text{-}Am)_4$	1.0	Yellow-red liquid	38
		B.P. 102°C/2 mm	1
$Sn(O\text{-}n\text{-}hexyl)_4$	1.2	Yellow liquid	38
$Sn(O\text{-}CHMe\text{-}n\text{-}Bu)_4$	1.0	Pale yellow solid	38
$Sn(O\text{-}cyclohexyl)_4$	1.4	Liquid	38
$Sn(O\text{-}Ph)_4$	1.4	Solid	38
$Sn(O\text{-}n\text{-}hept)_4$	1.0	Yellow liquid	38
$Sn(O\text{-}CHEt\text{-}n\text{-}Bu)_4$	1.0	Yellow-red liquid	38
$Sn(O\text{-}CEt_3)$	1.0	Yellow-red liquid	38
$Sn(O\text{-}n\text{-}Oct)_4$	1.0	Yellow-red liquid	38
$Sn(O\text{-}t\text{-}Bu)_4$	1.0	White solid	38
		B.P. 99°C/4.0 mm	1
		M.P. 39°C	42
$MSn(O\text{-}t\text{-}Bu)_5$ $M = K, Rb, Cs$	1.0	Solid	50
$[Sn(O\text{-}i\text{-}Pr)_4 \cdot HO\text{-}i\text{-}Pr]$	1.83(benzene)	White solid	42,51
	2.0(XRD)		37
$[Sn(O\text{-}i\text{-}Bu)_4 \cdot HO\text{-}i\text{-}Bu]$	2.0(XRD)	White solid	52,53

$[Sn(OR)_3(chel)]$, chel = acac
    R = ME
    R = Bu
    R = t-Bu
    R = i-Pr
			43

$[Sn(OR)_3(chel)]$, R = i-Pr
    chel = pvm
    chel = bzac
	2.0		43

$[((COD)Rh)_2Sn(OEt)_6]$	1.0(XRD)	Yellow solid	54
$[Tl_2Sn(OEt)_6]$	1.0(benzene) infinite polymer	White solid	55
$Cd_4Sn_4(\mu_4\text{-}O)_2$ $(O_2CCH_3)(ONp)_{10}$	1.0(XRD)	White solid	56

(b) Structural properties

(1) Tin(IV) alkoxide compounds There were very little structural data available for tin(IV) alkoxide compounds until fairly recently. NMR spectroscopy has not been extensively used to characterize these species, and very few examples have been characterized by single-crystal X-ray diffraction. This is surprising in view of the presence of two NMR active isotopes of tin which should significantly aid solution structural determination by NMR spectroscopy. Alkyl tin(IV) alkoxide compounds have been the subject of solution structural studies based on multinuclear NMR spectroscopy and molecular weight determination, particularly by Kennedy et al. [57]. They have suggested a variety of structures for a number of these species. The reader is referred to the original work for details, but some of the proposed structures are illustrated in Fig. 2 to provide insight into the structural variety and for comparison with other species.

A number of tin(IV) alkoxide species have more recently been characterized in the solid state by single crystal X-ray diffraction and in solution by NMR and IR spectroscopies.

Tin(IV) tertiary butoxide is monomeric in the solid state, consistent with molecular weight determinations in benzene solution [42]. An ORTEP view of Sn(O-t-Bu)$_4$ is shown in Fig. 3. The tetrahedral coordination environment of the tin(IV) center is distorted, O(2)–Sn–O(2') and O(7)–Sn–O(7') are enlarged ($\sim 115°$) while the other O–Sn–O angles are reduced (105° and 107°) compared with the tetrahedral angle. The Sn–O distances are 1.946 and 1.949 Å, slightly smaller than the sum of the Sn and O covalent radii. However, the Sn–O–C angles are 125.0(2)° and 124.1(2)° for O(2) and O(7), respectively, the region expected for the absence of π-donation from the alkoxide oxygen to the metal center.

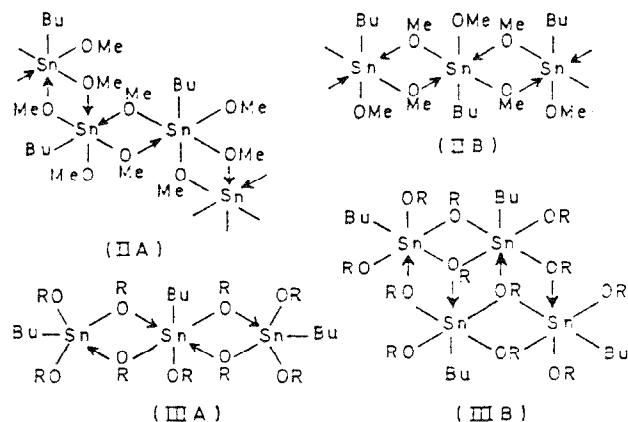Since this species contains only terminal tin alkoxide bonds both in the solid

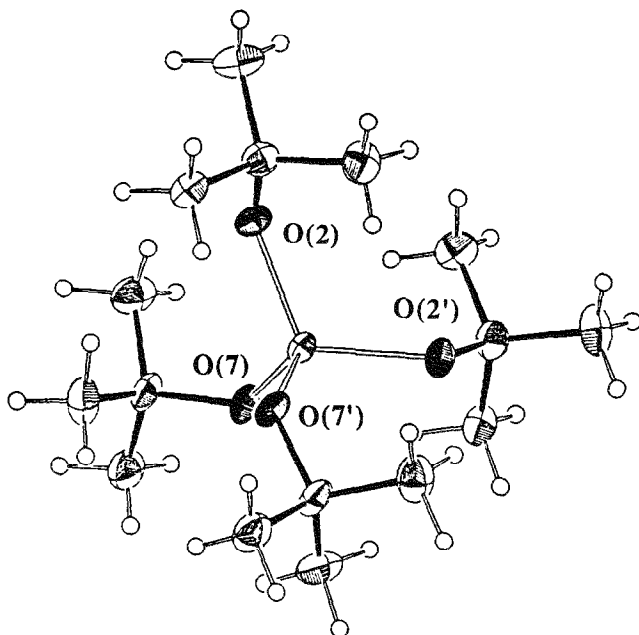Fig. 2. Structural variety proposed for alkyl tin(IV) alkoxide compounds [57].

Fig. 3. ORTEP plot of the solid state molecular structure of Sn(O-*t*-Bu)$_4$.

state and in solution, it has been used as a model compound to determine whether or not it is possible to develop criteria for the distinction of different tin–alkoxide ligand bonding modes (i.e. terminal versus doubly bridging versus triply bridging) in solution. It is particularly important to develop methods to determine structures in solution to gain further insight into sol–gel-type hydrolysis and condensation studies. In benzene solution, no coupling is observed between the two NMR active nuclei of tin (^{119}Sn 8.58% natural abundance, $I = 1/2$ and ^{117}Sn, 7.61% natural abundance, $I = 1/2$ [58]) with the single type of proton of the tertiary butoxide ligand observed by ^{1}H NMR spectroscopy. Coupling between the NMR-active tin isotopes and both types of carbon, however, can be observed by ^{13}C NMR spectroscopy with values of $^2J_{(^{119}Sn-O-C)} = 45$ Hz and $^3J_{(^{119}Sn-O-C-C)} = 27$ Hz. The values of the two bond tin–carbon coupling constant have been compared in a number of different tin(IV) alkoxide compounds and found to be a viable solution spectroscopic criterion for the distinction of terminal versus doubly bridging alkoxide ligands. The value of the two-bond tin–carbon coupling lies in the range 40–50 Hz for terminal tin alkoxide ligands, while that of doubly bridging alkoxide ligands lies in the range 20–30 Hz. Thus far, no homoleptic tin(IV) alkoxide compounds have been characterized that contain triply bridging alkoxide ligands in solution.

The ^{119}Sn NMR chemical shift of Sn(O-*t*-Bu)$_4$ has been reported by a number of workers at approximately -373 ppm upfield of SnMe$_4$ [42,43]. ^{119}Sn NMR spectroscopy is expected to provide a probe of the tin coordination number in tin

alkoxide compounds since correlations of ^{119}Sn chemical shift and coordination number have been made for various related groups of compounds [59]. A unit increase in coordination number causes a high field shift of the ^{119}Sn resonance of 120–150 ppm for coordination numbers 4–7 in a variety of different classes of compounds. This trend also seems to hold true for tin(IV) alkoxide compounds where octahedral homoleptic tin(IV) alkoxide compounds exhibit a ^{119}Sn chemical shift in the region -600 to -700 ppm. The ^{119}Sn chemical shift of a five-coordinate homoleptic tin(IV) alkoxide compound could therefore be predicted at ~ -400 to -500 ppm. This trend has been used to assign the coordination number in a series of (β-diketonate)$_n$Sn(OR)$_{4-n}$ compounds [43].

The potential of solid state ^{119}Sn NMR spectroscopy has yet to be exploited for the characterization of structure and dynamic processes of tin(IV) alkoxide compounds in the solid state. A number of publications have appeared on the use of solid state ^{119}Sn NMR spectroscopy for the characterization of tin oxide species, and it is noteworthy that, in BaSnO$_3$, the ^{119}Sn–O–^{117}Sn coupling could be observed [60]. The correlation between $^2J_{(^{119}Sn-X-^{117}Sn)}$ for X = chalcogenide and molecular structure has previously been investigated [61,62]. The solid state ^{119}Sn NMR of tin(IV) alkoxide compounds has the potential advantage, compared with tin oxides, that cross-polarization (CP) techniques could be used to reduce the total acquisition time for these experiments. The solid state ^{119}Sn NMR spectra of Sn(O-t-Bu)$_4$ shown in Fig. 4 were recorded under conditions of magic angle spinning (MAS) and of CP/MAS [63]. The signal-to-noise ratio is similar for both experiments, but the CP/MAS spectrum was obtained in approximately one tenth the time. The narrow linewidth is probably due to the high symmetry of the tin center in the tetrahedral
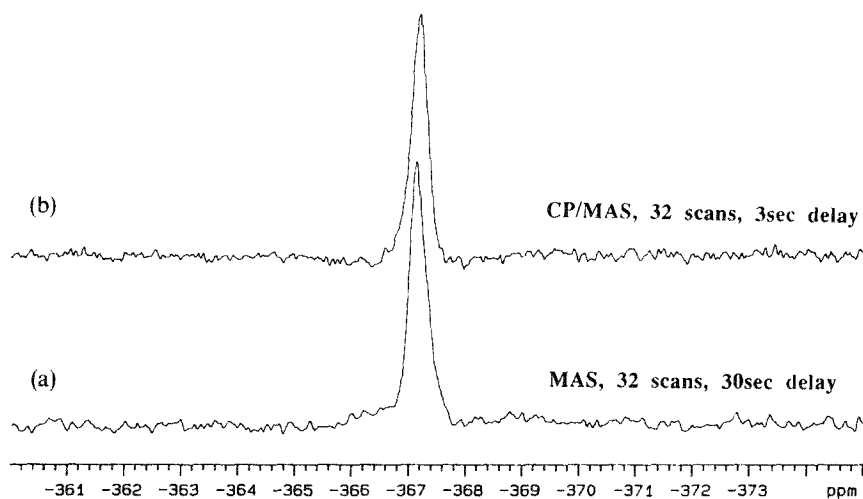

Fig. 4. Solid state ^{119}Sn NMR data for Sn(O-t-Bu)$_4$ recorded under conditions of (a) MAS and (b) CP/MAS.

environment of the four alkoxide ligands and results in small chemical shift anisotropy (CSA). In less symmetrical environments, the CSA is likely to be significantly larger and may obscure the presence of $^2J_{(^{119}Sn-OR-^{117}Sn)}$, which could provide valuable connectivity information.

The $\nu(M-O)$ stretching frequency for a variety of metal alkoxide compounds has been assigned to bands in the region 500–625 cm^{-1} [64]. The majority of data for tin(IV) alkoxide compounds comes from studies of alkyl tin(IV) alkoxide species. The tin–oxygen stretch has been assigned to the band observed at ~ 500 cm^{-1} in these compounds and empirical calculations predicted the $\nu(Sn-O)$ stretch at 570 cm^{-1}. The asymmetric $\nu_{as}(Sn-C)$ stretch appears in a similar region (500–600 cm^{-1}), and coupling between $\nu(Sn-O)$ and symmetric $\nu_s(Sn-C)$ modes has also been postulated [65]. As a result, it is difficult to make an unambiguous assignment based on these data. More recently [43], the infrared spectrum of Sn(O-t-Bu)$_4$ has been investigated as a simple example of a tin alkoxide compound in view of the presence of a single type of alkoxide ligand. A band observed at 605 cm^{-1} was tentatively assigned to $\nu(Sn-O)$. This assignment was confirmed by preparation of the deuterium-labelled analogue, Sn(O-t-Bu-d_9)$_4$, for which the band at 605 cm^{-1} was absent and a new intense band was observed at 568 cm^{-1}. Using a simplified "diatomic molecule" approach, the tin–oxygen stretching frequency in Sn(O-t-Bu-d_9)$_4$ was calculated to be ~ 580 cm^{-1} by treating the labelled and unlabelled tertiary butoxide ligands as point masses of 82 and 73 mass units, respectively. The new band assigned to $\nu(Sn-O)$ observed in Sn(O-t-Bu-d_9)$_4$ was at lower energy than predicted, but in the range expected based on this crude model. In addition, the position of $\nu(C-O)$ could also be assigned to 973 cm^{-1} in the unlabelled compound and 873 cm^{-1} in the deuterium-labelled compound.

Moving to species of higher molecular complexity, Lewis base adducts of tin(IV) isopropoxide [43], tin(IV) isobutoxide [52], and tin(IV) benzyl alkoxide [46] are all dimeric both in the solid state and in solution. The solid state structures of these derivatives have been determined by single-crystal X-ray diffraction. The ORTEP plots for [Sn(O-i-Pr)$_4$·HO-i-Pr]$_2$, [Sn(O-i-Bu)$_4$·HO-i-Bu]$_2$, and [Sn(O-Bz)$_4$·HNMe$_2$]$_2$ are shown in Figs. 5–7, respectively.

A related species that has also been structurally characterized in the solid state and which could be considered as a Lewis base adduct of a tin(IV) alkoxide is the species [(acac)Sn(O-i-Pr)$_3$]$_2$ [38]. The ORTEP plot for this species is shown in Fig. 8.

All four compounds exhibit a similar structure that can be described as edge-shared bioctahedral in which the two octahedral tin fragments are connected by two doubly bridging alkoxide ligands. The general structural framework is represented in Fig. 9. The solid state structures of [Sn(O-i-Pr)$_4$·HO-i-Pr]$_2$ and [Sn(O-i-Bu)$_4$·HO-i-Bu]$_2$ both contain two terminal alkoxide ligands at each tin in the same plane as the doubly bridging alkoxide ligands and a terminal alkoxide ligand perpendicular to this plane. In addition, perpendicular to the bridges, there is one alcohol ligand coordinated to each tin which is involved in asymmetric intramolecular hydrogen
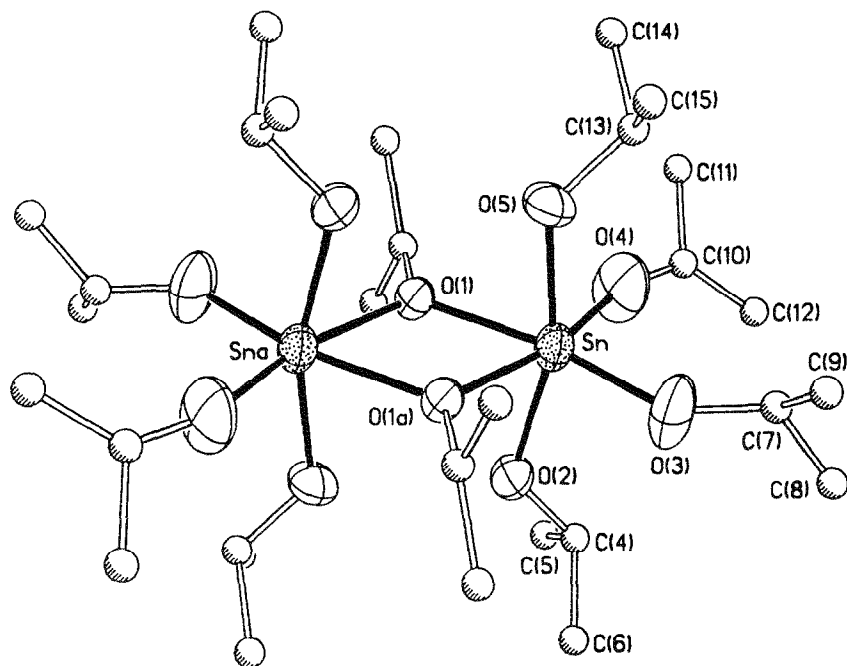
Fig. 5. ORTEP plot of the solid state molecular structure of $[Sn(O-i-Pr)_4 \cdot HO-i-Pr]_2$.

bonding to an alkoxide ligand of the adjacent tin atom. The asymmetry in the hydrogen bridge is evident from the difference in the coordination of alcohol and alkoxide ligands to the metal centers. Similar solid-state structures have recently been observed for the species $[M(O-i-Pr)_4 \cdot HO-i-Pr]_2$, where $M = Zr$, Hr, and Ce. This is quite reasonable since the covalent radii of the tetravalent Sn, Zr, Hf, and Ce atoms are quite similar [66]. In contrast, while titanium(IV) is only slightly smaller than tin(IV), the size difference is sufficient to cause a distinct difference in its metal alkoxide coordination chemistry. Thus, titanium(IV) isopropoxide does not form an isopropanol adduct, and is monomeric in benzene solution; whereas, in the absence of excess isopropanol, tin(IV) isopropoxide is believed to be trimeric.

The solid-state structures of $[Sn(O-i-Pr)_4 \cdot HO-i-Pr]_2$ and $[Sn(O-i-Bu)_4 \cdot HO-i-Bu]_2$ are not retained in solution at room temperature [43,52]. In benzene solution, $[Sn(O-i-Pr)_4 \cdot HO-i-Pr]_2$ exhibits only one type of OR ligand as determined by ^1H and ^{13}C NMR spectroscopy at room temperature, indicating a rapid exchange on these time scales. Cryoscopic molecular weight determination data measured at about $5°C$ reveal that the molecular complexity is 1.8. In the ^{119}Sn NMR spectrum, a single resonance is observed at -648 ppm upfield of $SnMe_4$, consistent with an average octahedral tin(IV) environment, together with ^{117}Sn satellites with an intensity and coupling constant consistent with a dimeric core of tin atoms. Upon cooling to $-20°C$, the ^{13}C NMR data reveal the decoalescence of the ^{13}C isopropoxide environ-
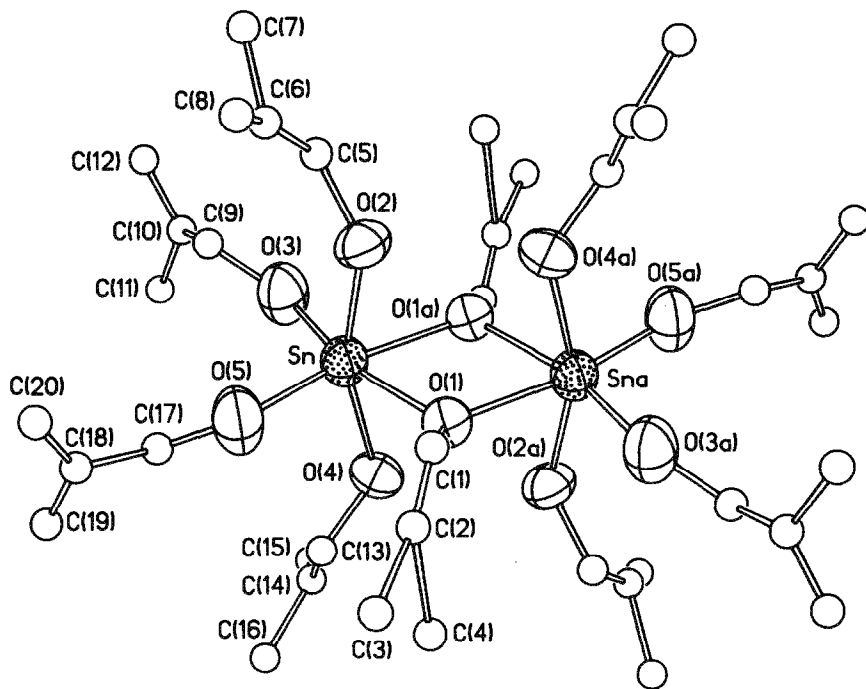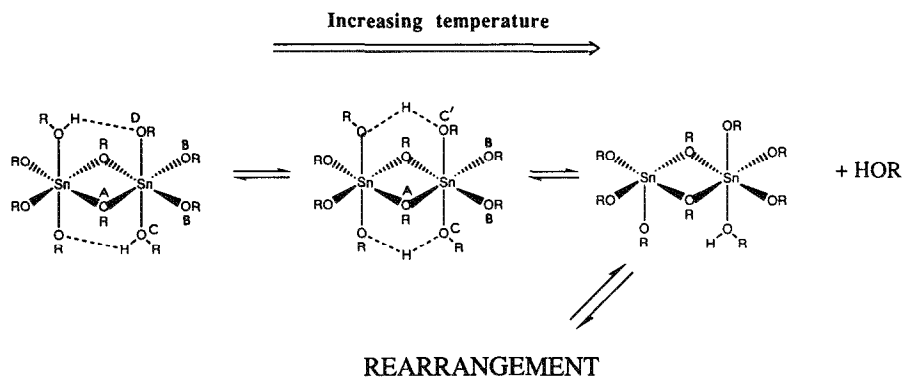
Fig. 6. ORTEP plot of the solid state molecular structure of $[Sn(O\text{-}i\text{-}Bu)_4 \cdot HO\text{-}i\text{-}Bu]_2$.

ments to give three resonances in the ratio $1:2:2$. At the same time, the ^1H NMR resonance of the alcoholic proton exhibits a triplet multiplicity. Taken together, these data are consistent with the presence of a species with D_{2h} symmetry, as shown in Scheme 1, in which the alcoholic proton undergoes rapid intramolecular exchange between the terminal alkoxide ligand and the coordinated alcohol. Upon further

Scheme 1. Proposed solution dynamic rearrangement process observed for $[Sn(O\text{-}i\text{-}Pr)_4 \cdot HO\text{-}i\text{-}Pr]_2$ as a function of temperature in toluene solution.
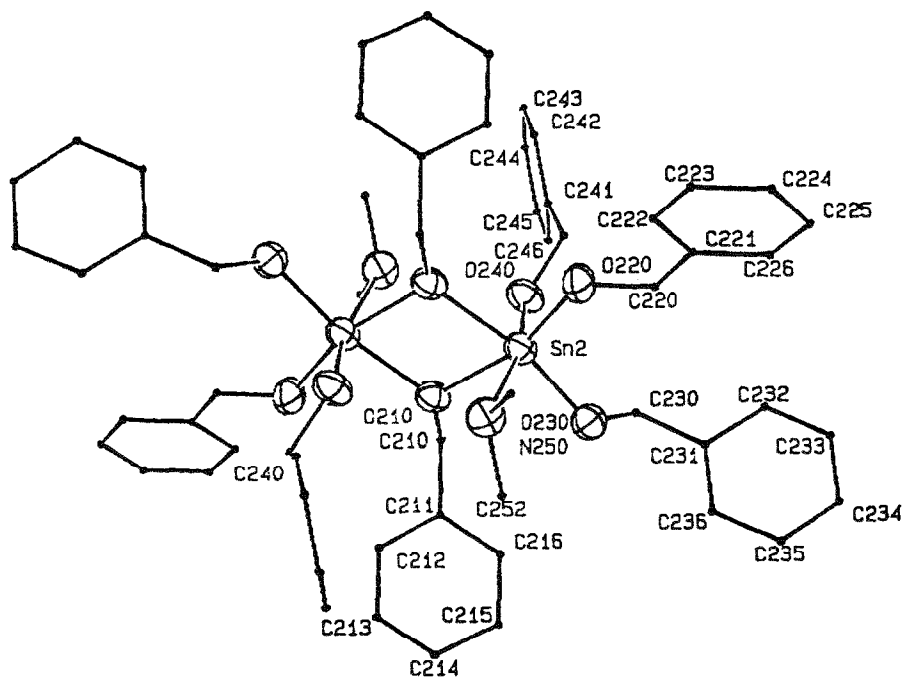
Fig. 7. ORTEP plot of the solid state molecular structure of [Sn(O-Bz)$_4 \cdot$HNMe$_2$]$_2$.

cooling, one of the ^{13}C resonances of relative intensity two decoalesces to form two resonances of equal intensity. These data are consistent with the localized asymmetric hydrogen bond and the C_{2h} structure shown in Scheme 1, analogous to the solid state structure of this compound. The activation barrier for the intramolecular proton exchange process estimated from the ^{13}C NMR coalescence data is $<11.9 \pm 0.5$ kcal mol^{-1}. This value is significantly larger than the enthalpy of hydrogen bonds in carboxylic acids, for example, but the exchange process in this case is probably associated with quite a large degree of steric and electronic rearrangement.

The compound [Sn(O-i-Bu)$_4 \cdot$HO-i-Bu]$_2$ exhibits [52] the D_{2h} structure in benzene solution at room temperature as determined by ^{1}H, ^{13}C and ^{119}Sn NMR spectroscopy and is dimeric according to cryoscopic molecular weight determination. The diagnostic utility of the $^2J_{(^{119}Sn-O-^{13}C)}$ coupling constant in the distinction of terminal versus doubly bridging alkoxide ligands is exemplified by this species and is illustrated diagrammatically in Scheme 2. Unlike [Sn(O-i-Pr)$_4 \cdot$HO-i-Pr]$_2$, [Sn(O-i-Bu)$_4 \cdot$HO-i-Bu]$_2$ does not appear to dissociate HO-i-Bu in solution even at elevated temperatures.

The molecular structure of [Sn(OBz)$_4 \cdot$HNMe$_2$]$_2$ is analogous to the isopropoxide and isobutoxide species just described except that the position of coordination of the alcohol ligand is now occupied by dimethylamine [46]. The orientation of the benzylalkoxide and coordinated amine ligand, in the plane perpendicular to that
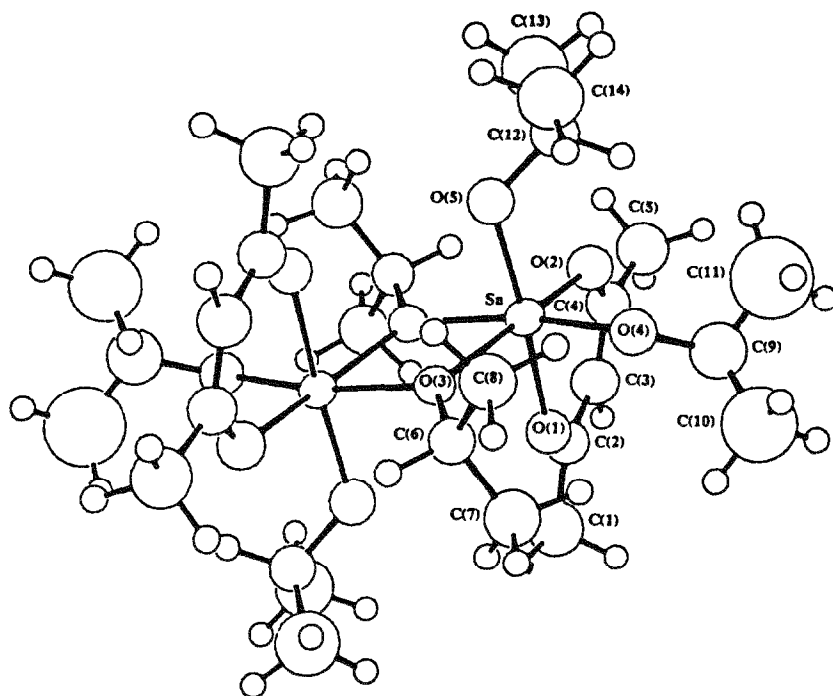
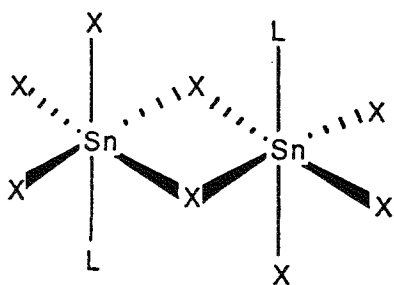Fig. 8. ORTEP plot of the solid state molecular structure of [Sn(O-i-Pr)$_3$(acac)]$_2$.

Fig. 9. Schematic representation of the edge-shared bioctahedral framework of the Sn$_2$X$_8$L$_2$.

containing the doubly bridging alkoxide ligands, is such that asymmetric hydrogen bonding may occur in the solid state.

The solid-state structure of [Sn(acac)(O-i-Pr)$_3$]$_2$ is analogous to the other members of this class described above in that one of the oxygen atoms of the β-diketonate ligand occupies a terminal position in the plane of the doubly bridging alkoxide ligands. The other oxygen atom occupies the position that the neutral Lewis base does in the other complexes. In CDCl$_3$ solution, NMR data indicate that this species also undergoes structural reorganization at room temperature. ^{119}Sn NMR data reveal that structural reorganization occurs immediately upon dissolution in
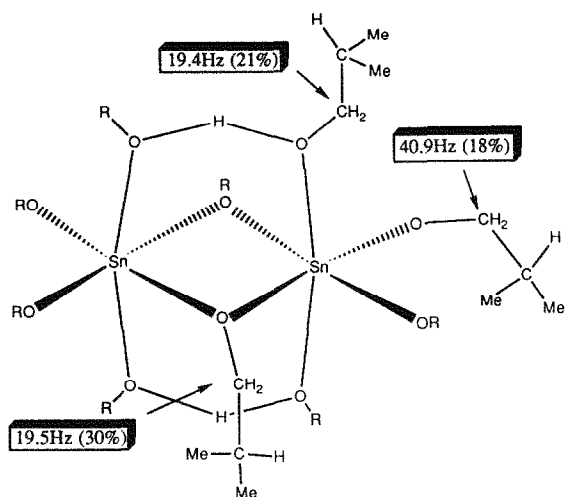
Scheme 2. Diagramatic representation of the use of $^2J_{(^{119}Sn-O-^{13}C)}$ coupling constant for assignment of different alkoxide bonding modes in $[Sn(O\text{-}i\text{-}Bu)_4 \cdot HO\text{-}i\text{-}Bu]_2$.
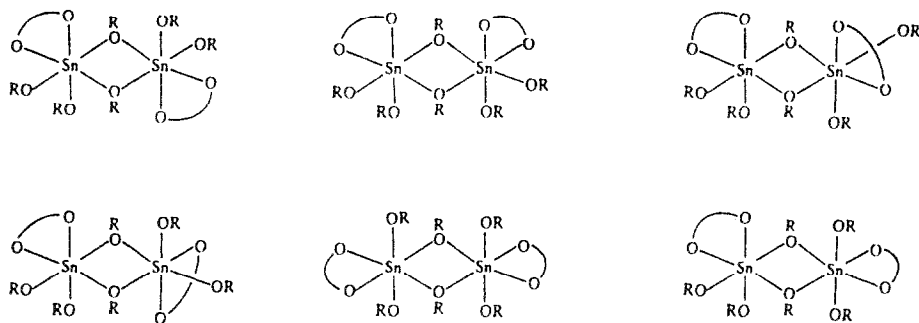
Scheme 3. Possible isomers formed via structural reorganization of $[Sn(O\text{-}i\text{-}Pr)_3(\beta\text{-diketonate})]_2$ in $CDCl_3$ solution.

$CDCl_3$, and, in addition, ligand redistribution occurs over a period of hours, possibly according to the stoichiometry of the equation

$$2[Sn(acac)(O\text{-}i\text{-}Pr)_3] \rightarrow [Sn(acac)_2(O\text{-}i\text{-}Pr)_2] + [Sn(O\text{-}i\text{-}Pr)_4] \qquad (18)$$
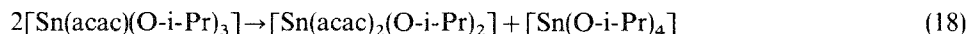
Intramolecular structural reorganization of $[Sn(\beta\text{-diketonate})(O\text{-}i\text{-}Pr)_3]_2$ may occur via opening of the bridging alkoxide ligands to give a variety of structural possibilities such as those shown below proposed by Chandler et al. [43].

An oligomeric species has been structurally characterized in the solid state derived from the reaction of $SnCl_4$ with two equivalents of triethanolamine [67]. This species possesses a monomeric octahedral tin(IV) coordination environment consisting of four alkoxide ligands in the same plane and two trans nitrogen atom

donors of each of the triethanolamine molecules. The remaining pendant alcohol ligands are hydrogen bonded to adjacent molecules in a direction parallel to the molecular two-fold axis of symmetry to form an infinite hydrogen bonded polymer. The structure is depicted schematically in Fig. 10. This species has been isolated and characterized in two different forms. The difference between these forms is the way the molecules are hydrogen bonded to each other in the solid state [68]. Unfortunately, there is no solution structural data available for this species at present.

A number of other mixed ligand–tin(IV) alkoxide species, such as $Sn(NMe_2)_2(OAr)_2$, have been structurally characterized in the solid state recently but these species are beyond the scope of this review [40,41].

(2) Mixed metal tin(IV) alkoxide compounds   A number of examples of mixed metal tin(IV) alkoxide compounds have been reported in the literature. A summary of their relevant structural features are presented here.

The thallium(I)–tin(IV) alkoxide compound $Tl_2Sn(OEt)_6$ has been isolated from the reaction of two equivalents of thallium(I) ethoxide and tin(IV) ethoxide [55] according to

$$2TlOEt + Sn(OEt)_4 \rightarrow [Tl_2Sn(OEt)_6] \tag{19}$$

In the solid state, $Tl_2Sn(OEt)_6$ exists as a one-dimensional, infinite polymer with two types of alkoxide ligand as shown in Fig. 11. There are two doubly bridging alkoxide ligands that bridge thallium and tin and one type of triply bridging ethoxide ligand that bridges two thallium centers and one tin atom. These polymer chains stack in a parallel fashion along the *c*-axis of the crystal, as shown in Fig. 12. Each tin(IV) center exists in an octahedral coordination environment, while each thallium is probably best considered as distorted trigonal bipyramid, with a lone pair occupying the vacant equatorial coordination site. In solution, this compound is monomeric, according to cryoscopic molecular weight determination in benzene solution, and exhibits a single type of ethoxide ligand over a temperature range -90 to $+25°C$, according to ^1H and ^{13}C NMR spectroscopy. The methylene ^{13}C NMR resonance of the ethoxide ligands exhibits a two bond $J_{(^{119}Sn-O-C)}$ coupling constant consistent with the presence of doubly bridging ethoxide ligands. The ^{119}Sn chemical shift of
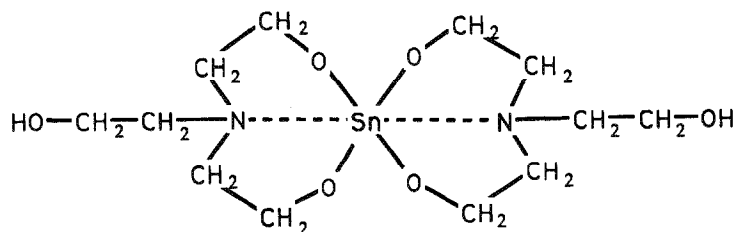

Fig. 10. Molecular structure of $Sn[(OCH_2CH_3-N(CH_2CH_2OH)]_2$.
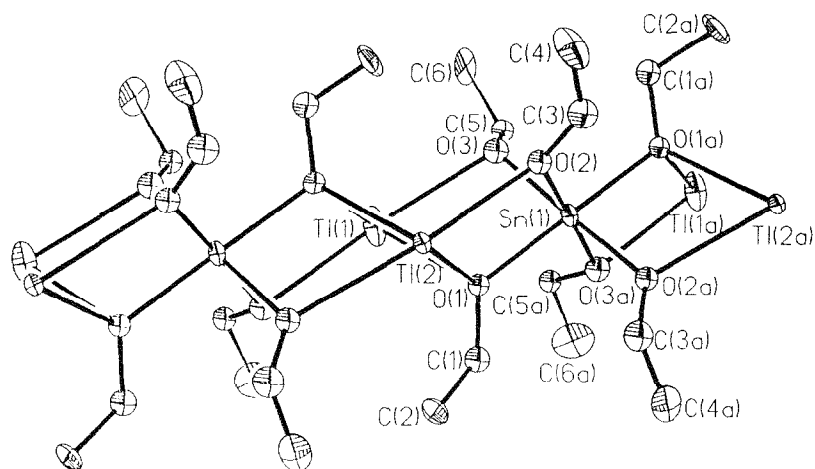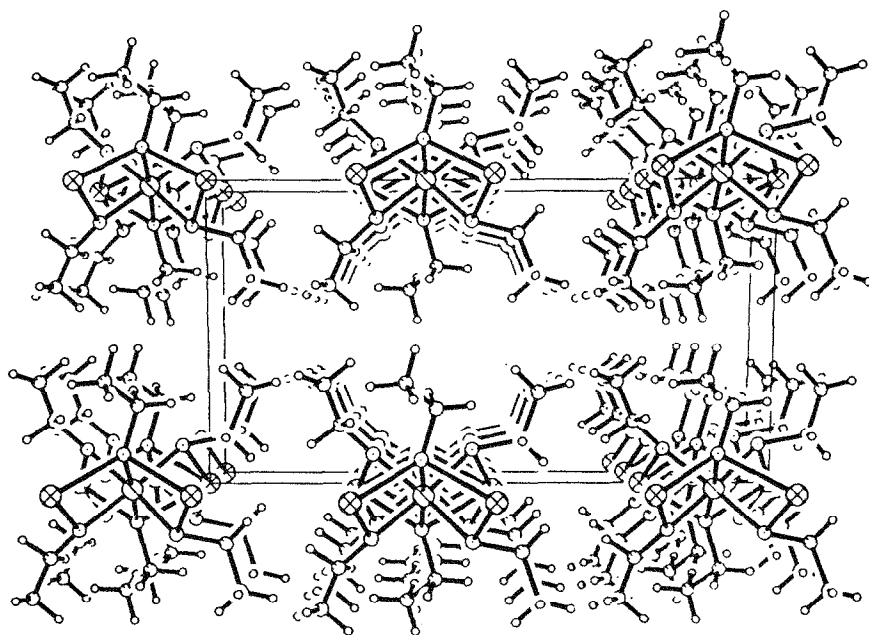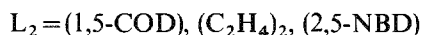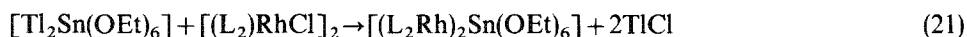
Fig. 11. ORTEP plot of the molecular structure of $TlSn(OEt)_6$.

Fig. 12. ORTEP plot of the crystal structure of $[Tl_2Sn(OEt)_6]_n$.

-596 ppm is consistent with an octahedral coordination number. It seems unlikely that this species undergoes a dynamic rearrangement in solution since exchange with either added excess ethanol or thallium ethoxide was not observed. The compound $Tl_2Sn(OEt)_6$ exhibits a single $\nu(Sn-O)$ stretch in the infrared spectrum at 528 cm^{-1} in the solid state that moves to 541 cm^{-1} in toluene solution. Both positions are

lower than those observed for terminal alkoxide ligands of $Sn(O\text{-}t\text{-}Bu)_4$. Although the solution structure was not unambiguously established, the covalent monomeric structure shown in Fig. 13 was postulated and is similar to that observed for $[TlSn(O\text{-}t\text{-}Bu)_3]$ and $Pb(O\text{-}t\text{-}Bu)_2$ [69].

The compound $Tl_2Sn(OEt)_6$ can be used as a source of $[Sn(OEt)_6]^{2-}$ and, under appropriate conditions, reacted with metal halides as a route for the synthesis of other mixed metal alkoxide compounds. Two examples are presented in the equations [70]

$$[Tl_2Sn(OEt)_6] + ZnCl_2 \rightarrow ZnSn(OEt)_6 + 2TlCl \tag{20}$$

$$[Tl_2Sn(OEt)_6] + [(L_2)RhCl]_2 \rightarrow [(L_2Rh)_2Sn(OEt)_6] + 2TlCl \tag{21}$$

$$L_2 = (1,5\text{-COD}), (C_2H_4)_2, (2,5\text{-NBD})$$

Structural data for $ZnSn(OEt)_6$ have not been reported; however, $[((1,5\text{-COD})Rh)_2Sn(OEt)_6]$ has been structurally characterized in the solid state [54], and a number of the $[(L_2Rh)_2Sn(OEt)_6]$ derivatives have been characterized in solution. The solid-state structure of $[((1,5\text{-COD})Rh)_2Sn(OEt)_6]$ is shown in Fig. 14. The structure of $[((1,5\text{-COD})Rh)_2Sn(OEt)_6]$ consists of a tin(IV) center in an octahedral coordination environment of alkoxide ligands. Two of the cis edges of the octahedron are coordinated to two, square planar d^8 $[(1,5\text{-COD})Rh]^+$ moieties. The two remaining alkoxide ligands are terminal, resulting in a molecule with approximate C_2 molecular symmetry. There is a distortion of the octahedral coordination about tin $(O(3)\text{–}Sn\text{–}O(4) = 73.4°$ and $O(1)\text{–}Sn\text{–}O(2) = 74.4°)$ as a result of the coordination to the two rhodium cations. The angle between the cis-terminal alkoxide ligands is $90.4°$.

In solution, this species is monomeric at room temperature and exhibits only one type of ethoxide and cyclo-octadiene ligands, inconsistent with the solid-state structure. Upon cooling to $-90°C$ in toluene-d_8 solution, the ^1H NMR resonances of the ethoxide and cyclo-octadiene ligands broaden, but the low-temperature limiting spectrum could not be reached. However, for the carbonyl derivative, $[((CO)_2Rh)_2Sn(OEt)_6]$, one type of ethoxide ligand was observed at room temperature (with $^{119}Sn/^{117}Sn$ satellites), and the low-temperature-limiting ^1H and ^{13}C NMR spectra could be obtained. At $-80°C$, three types of alkoxide ligand were observed in the
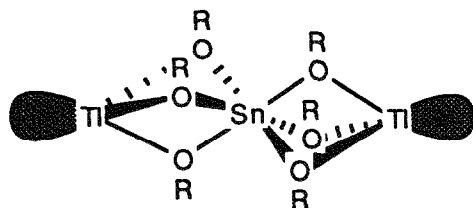

Fig. 13. Proposed solution structure of $[Tl_2Sn(OEt)_6]$.
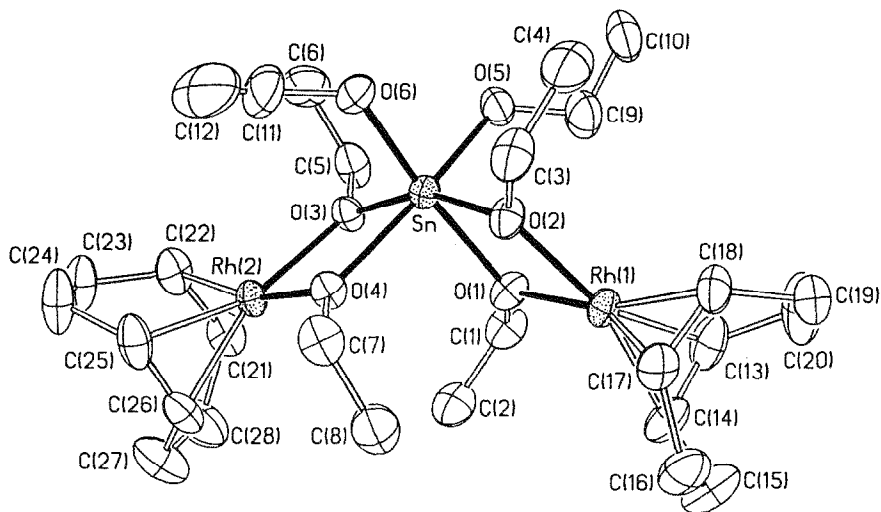
Fig. 14. ORTEP plot of the solid state molecular structure of [((1,5-COD)Rh)$_2$Sn(OEt)$_6$].

same ratio where all the methylenic protons were diastereotypic, according to the ^{1}H NMR data. This spectrum is consistent with a structure analogous to that adopted in the solid state for [((1,5-COD)Rh)$_2$Sn(OEt)$_6$]. At $-60°$C in the ^{13}C spectrum, one of the methylenic ethoxide carbon resonances exhibited a $^2J_{(^{119}Sn-O-^{13}C)}$ coupling constant of 40 Hz, consistent with a terminal ethoxide ligand, while the other two types exhibited couplings of <30 Hz in the range expected for doubly bridging ethoxide ligands. Furthermore, at room temperature during rapid exchange, the ^{13}C NMR resonance of the 99% ^{13}CO-enriched analogue reveals the presence of coupling to both ^{103}Rh and $^{119/117}$Sn and is consistent with an *intra*-molecular dynamic rearrangement process. It seems most likely that the species [((L$_2$)Rh)$_2$Sn(OEt)$_6$] undergoes a rapid, associative (five-coordinate rhodium) intra-molecular exchange at room temperature.

Addition of one equivalent of [(1,5-COD)Rh]$^+$ cation to [((1,5-COD)Rh)$_2$ Sn(OEt)$_6$] results in formation of the cation [((1,5-COD)Rh)$_3$Sn(OEt)$_6$]$^+$ according to the equation [71]

$$[((COD)Rh)_2Sn(OEt)_6] + [(COD)Rh]^+PF_6^- \rightarrow [((COD)Rh)_3Sn(OEt)_6]^+PF_6^- \qquad (22)$$
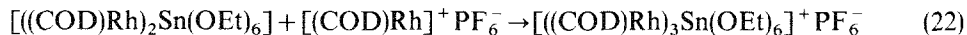
This species exhibits ^{1}H and ^{13}C NMR data consistent with formation of the symmetrical geometry shown in Fig. 15. Whether [((1,5-COD)Rh)$_3$Sn(OEt)$_6$]$^+$ undergoes degenerate dynamic rearrangement in solution is not known.

Vcith and coworkers, who have synthesized and characterized a large number of tin(II) alkoxide compounds [72–74], have recently turned their attention to tin(IV) alkoxide species [50]. The reaction of alkali metal tertiary butoxides of K, Rb, and Cs with Sn(O-t-Bu)$_4$ resulted in formation of the corresponding double alkoxide

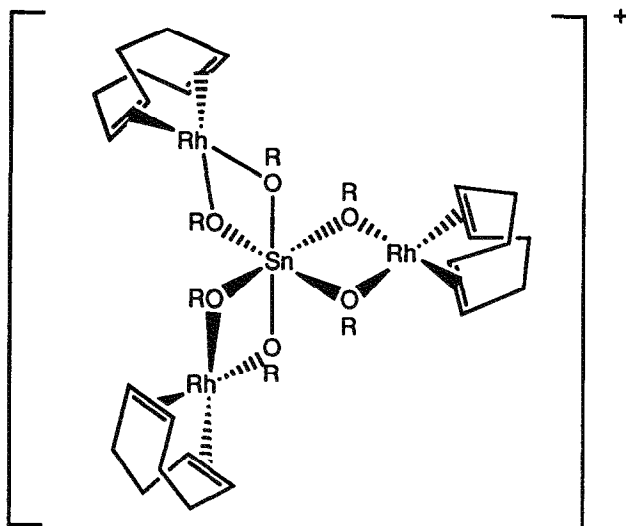Fig. 15. Proposed solution structure of $[((1,5\text{-}COD)Rh)_3Sn(OEt)_6]^+$.

compounds $[MSn(O\text{-}t\text{-}Bu)_5]$. Interestingly, while lithium and sodium tertiary butoxides react with tin(II) tertiary butoxide, no double alkoxide product was formed upon reaction of lithium or sodium tertiary butoxides with tin(IV) tertiary butoxide.

The derivative $[KSn(O\text{-}t\text{-}Bu)_5]$ was characterized in the solid state by single-crystal X-ray diffraction (Fig. 16). These data reveal that this compound exists as a helical polymer, with the tin atom coordinated to five other tertiary butoxide ligands in a trigonal bipyramidal coordination environment. Two pairs of the alkoxide ligands are also coordinated to two structurally inequivalent potassium ions, resulting in an approximately tetrahedral coordination environment for potassium. The remaining tertiary butoxide ligand coordinated to tin(IV) is terminal. In solution, molecular weight measurements determined cryoscopically in benzene reveal that
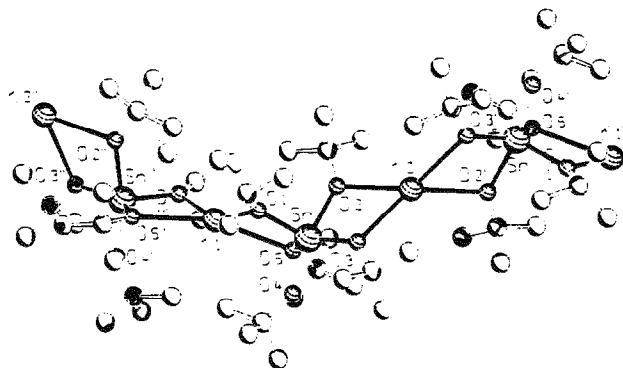

Fig. 16. ORTEP plot of the solid state molecular structure of $KSn(O\text{-}t\text{-}Bu)_5$.

both the potassium and the cesium derivatives are approximately monomeric. For [KSn(O-*t*-Bu)$_5$], only one type of alkoxide ligand was observed at room temperature by ^{1}H and ^{13}C NMR spectroscopy, and no change was observed upon cooling to $-90°$C. In the ^{13}C NMR spectrum, the two bond $^2J_{(^{13}C-O-^{119}Sn)}$ coupling constant of 47 Hz was consistent with the presence of terminal alkoxide ligands in solution. It is also noteworthy that the ^{119}Sn chemical shift of [KSn(O-*t*-Bu)$_5$] is significantly shielded compared with tetrahedral Sn(O-*t*-Bu)$_4$ [70]. The ^{119}Sn chemical shift of [KSn(O-*t*-Bu)$_5$] was observed at -588 ppm, approximately 215 ppm upfield of the value reported for Sn(O-*t*-Bu)$_4$ and about 60 ppm downfield of the value of [Sn(O-i-Pr)$_4$·HO-i-Pr]$_2$ with an octahedral tin(IV) coordination sphere. The ^{119}Sn NMR chemical shift is further upfield than the value expected for a five-coordinate homoleptic tin(IV) alkoxide compound, but this may be the result of significant (negative) charge localization on tin.

.A number of other mixed metal alkoxide species containing tin(IV) have been prepared, including Sn[Al(O-i-Pr)$_4$]$_4$, which is claimed to have an eight-coordinate tin environment [75], but structural characterization data have not been reported.

A number of metal-organic species have recently been isolated and structurally characterized with mixed ligand systems. These species have mainly been related to the superconducting or perovskite phase metal oxide ceramics. One example of a mixed ligand tin(IV) containing species, [Cd$_4$Sn$_4$(μ_4-O)$_2$(OAc)$_{10}$(O–Np)$_{10}$], has recently been isolated from the reaction of tin(IV) neopentoxide with cadmium acetate [56]. The single crystal X-ray diffraction structure of this species is shown in Fig. 17. The molecule contains a central planar eight-membered Cd$_4$O$_4$ ring. Two of the oxygen atoms in the eight-membered ring are μ_4-oxo groups and are each coordinated to two octahedral tin centers. The two other oxygens in the Cd$_4$O$_4$ ring are derived from one oxygen from each of two acetate ligands, the other oxygen of which is coordinated to another Cd. Two cadmium ions possess an approximately octahedral coordination environment, while the other two are seven-coordinate. Each cadmium is coordinated to an acetate group in a "coat-hanger" fashion above and below the Cd$_4$O$_4$ plane. Solution structural data for this species have not yet been reported. The origin of the oxo species has not been determined, but could arise as a result of esterification of the metal alkoxide compound.

Based on the single crystal X-ray diffraction data now available for tin(IV) alkoxide compounds, it should be possible to delineate some structural trends. Tabulation of the Sn–O distance for different modes of coordination of the alkoxide ligands, together with the Sn–O–C angles at oxygen for the terminal alkoxide ligands are presented in Table 2. While the standard deviation of some of the bond length data are fairly large, some trends are discernible. For the less sterically demanding alkoxide ligands, such as –OEt, –O-i-Pr, and –O-i-Bu, the difference in Sn–O bond length between terminal and doubly bridging alkoxide ligands is about 0.1 Å, and between terminal and triply bridging alkoxide ligands it is 0.13 Å (this may not be general since it is based on a single measurement).
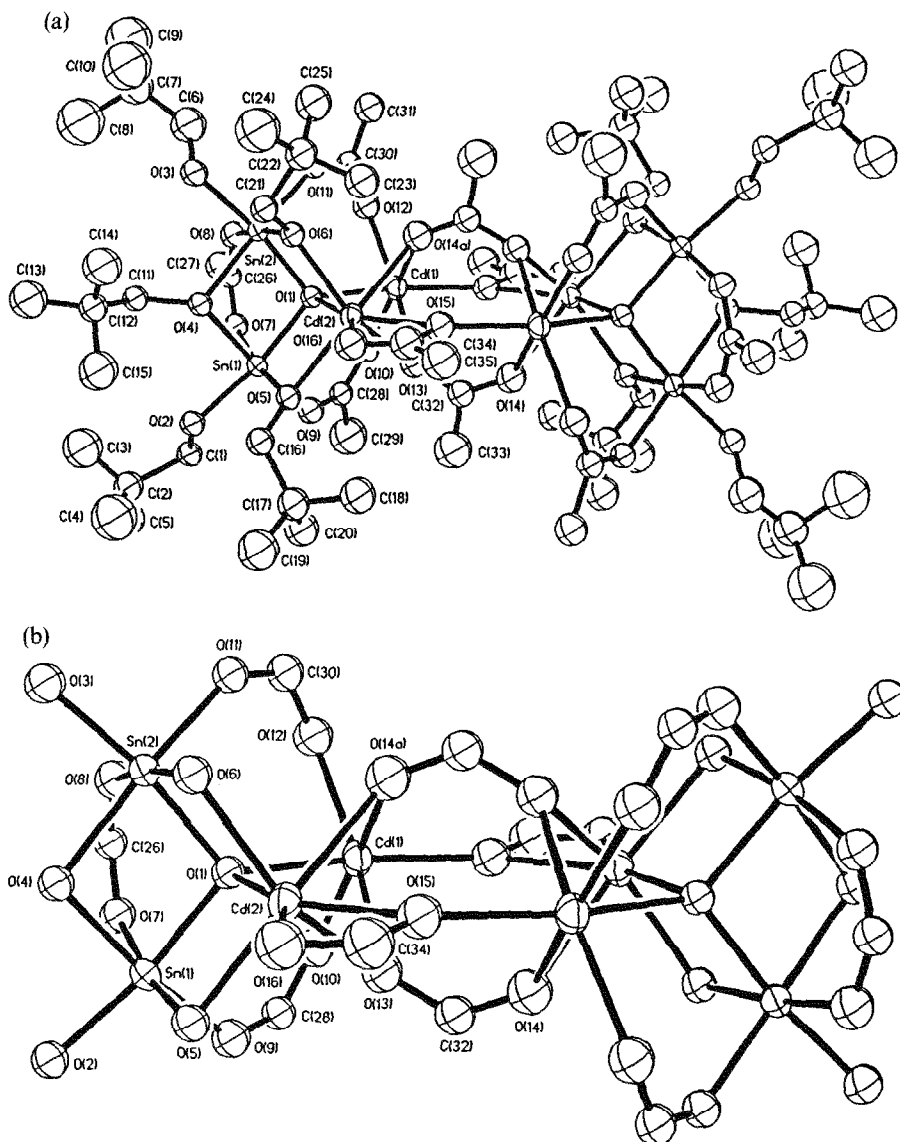
Fig. 17. ORTEP plot of the molecular structure of $[Cd_4Sn_4(\mu_4\text{-}O)_2(OAc)_{10}(O\text{-}Np)_{10}]$. (a) Hydrogen atoms omitted for clarity. (b) Core structure emphasizing metal atom coordination geometry.

Plots of Sn–O bond length versus Sn–O–C angle are shown in two different representations in Figs. 18 and 19. Figure 18 emphasizes this relationship as a function of the nature of the alkoxide binding mode (i.e. terminal versus doubly bridging). Figure 19 emphasizes this relationship as a function of the alkyl group. There appear to be no discernible trends as a function of the nature of the alkoxide

TABLE 2

Compilation of Sn–O bond length and Sn–O–C bond angle data for tin(IV) alkoxide compounds as a function of the nature of the alkoxide ligand and their bonding modes

Alkoxide type	M–O distance	Sn–O–C angle	Compound	Ref.
Sn-O-t-Bu	1.946(2)	125.0(2)	$Sn(O\text{-}t\text{-}Bu)_4$	42
	1.949(2)	124.1(2)		
	2.005(8)	141.7(8)	$KSn(O\text{-}t\text{-}Bu)_5$	50
μ^2-O-t-Bu	1.979(7)	128.1(7)	$KSn(O\text{-}t\text{-}Bu)_5$	50
	2.057(7)	136.6(7)		
	2.008(7)	133.4(7)		
	2.002(7)	126.5(7)		
Sn-O-i-Pr	1.964(7)	139.4(8)	$[Sn(O\text{-}i\text{-}Pr)_4 \cdot HO\text{-}i\text{-}Pr]_2$	42
	1.923(7)	160.0(9)		
	1.957(7)	122.0(5)	$[Sn(O\text{-}i\text{-}Pr)_3(acac)]_2$	43
	1.974(3)	124.4(4)		
μ^2-O-i-Pr	2.080(4)	124.1(5)	$[Sn(O\text{-}i\text{-}Pr)_4 \cdot HO\text{-}i\text{-}Pr]_2$	42
	2.098(6)	126.5(5)		
	2.079(4)	128.1(3)	$[Sn(O\text{-}i\text{-}Pr)_3(acac)]_2$	43
Sn⋯O(H)-i-Pr	2.142(6)	128.5(5)	$[Sn(O\text{-}i\text{-}Pr)_4 \cdot HO\text{-}i\text{-}Pr]_2$	42
O-i-Bu	1.943	128.7	$[Sn(O\text{-}i\text{-}Bu)_4 \cdot HO\text{-}i\text{-}Bu]_2$	52
	1.932	131.9		
μ^2-O-i-Bu	2.094	123.0	$[Sn(O\text{-}i\text{-}Bu)_4 \cdot HO\text{-}i\text{-}Bu]_2$	52
	2.069	122.1		
	2.108	126.6		
Sn⋯O(H)-i-Bu	2.114	121.7	$[Sn(O\text{-}i\text{-}Bu)_4 \cdot HO\text{-}i\text{-}Bu]_2$	52
Sn-O-Et	1.979(5)	125.4(5)	$[((COD)Rh)_2Sn(OEt)_6]$	54
	1.980(4)	127.6(5)		
μ^2-O-Et	2.098(3)	124.4(3)	$[((COD)Rh)_2Sn(OEt)_6]$	54
	2.075(4)	122.5(3)		
	2.082(4)	123.5(4)		
	2.103(4)	125.9(4)		
	2.023(3)	129(3)	$[Tl_2Sn(OEt)_6]$	55
	2.05(4)	125(3)		
μ^3-O-Et	2.11(2)	121(2)	$[Tl_2Sn(OEt)_6]$	55
Sn-O-Np	1.97(2)	119(2)	$Cd_4Sn_4(\mu_4\text{-}O)_2(O_2CCH_3)(ONp)_{10}$	56
μ^2-O-Np	2.00(2)	125(1)	$Cd_4Sn_4(\mu_4\text{-}O)_2(O_2CCH_3)(ONp)_{10}$	56
	2.10(2)	123(1)		

ligand. The terminal Sn–O bond lengths lie between 1.95 and 2.0 Å, while the $\mu\text{-}^2$(OR) bond lengths lie in the region 2.0–2.1 Å, approximately 0.1 Å longer. The Sn–O–C angles all lie in the region 120°–140° with the exception of one of the terminal Sn–O-i-Pr ligands of $[Sn(O\text{-}i\text{-}Pr)_4 \cdot HO\text{-}i\text{-}Pr]_2$, which exhibit an unusually short and unusually linear coordination. The corresponding metrical parameters for $[Sn(O\text{-}i\text{-}Bu)_4 \cdot HO\text{-}i\text{-}Bu]_2$ are Sn–O = 1.93 Å and Sn–O–C = 132°. It is interesting to
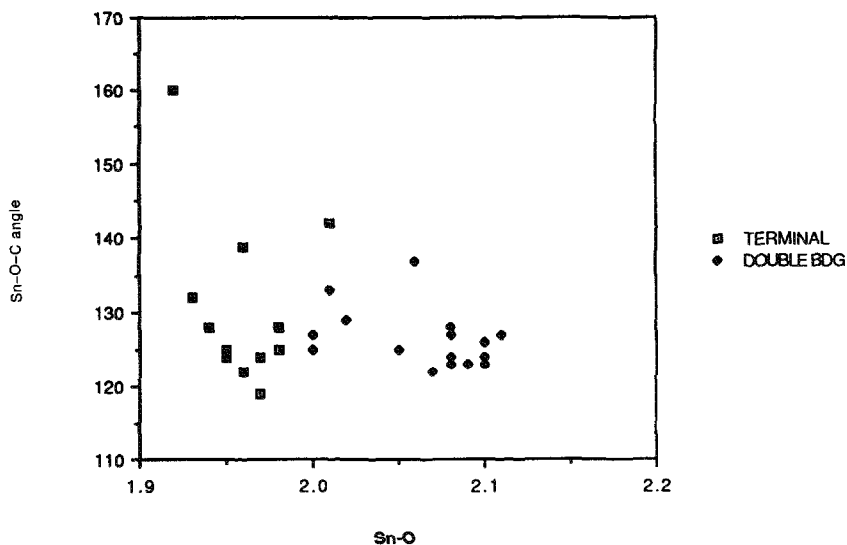
Fig. 18. Plot of Sn–O bond length vs. Sn–O–C angle as a function of bonding mode.
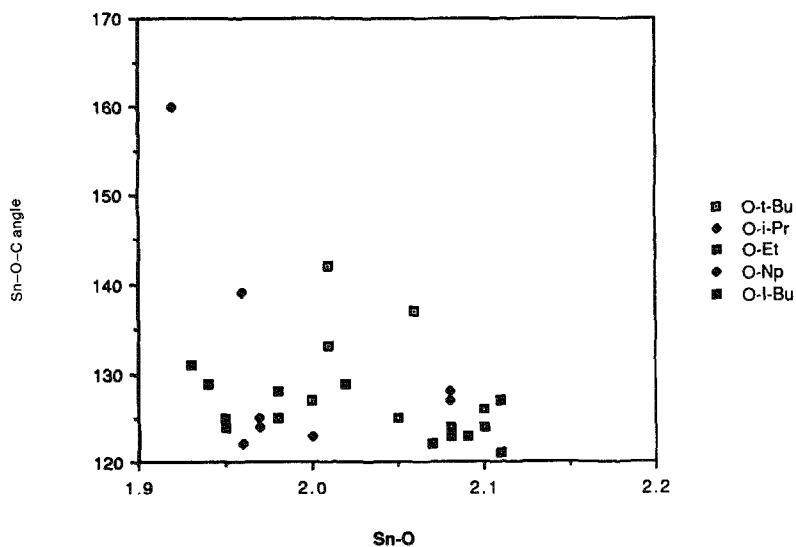
Fig. 19. Plot of Sn–O bond length vs. Sn–O–C angle as a function of alkoxide type.

compare this result with the analogous distances and angles of the isostructural compounds $[M(O\text{-}i\text{-}Pr)_4 \cdot HO\text{-}i\text{-}Pr]_2$ which are $M = Zr$, 177° and 167° and for $M = Ce$, 172° and 167°.

These data may be useful for development of bond length–bond strength relationships in tin(IV) alkoxide compounds and used to predict the relative thermo-

dynamic stability of terminal versus doubly bridging versus triply bridging alkoxide compounds with respect to hydrolysis.

As noted in the Introduction, while the hydrolysis and condensation of silicon alkoxides have been extensively studied, only a relatively small number of studies have been aimed at deriving an understanding of the hydrolysis and condensation of other metal alkoxide compounds [16]. There are even fewer studies of the tin(IV) alkoxide system, even though many patents have been issued on the use of tin(IV) alkoxide compounds as precursors to form SnO_2.

Bradley and Holloway [51] studied the controlled hydrolysis of tin(IV) isopropoxide, $[Sn(O\text{-}i\text{-}Pr)_4 \cdot HO\text{-}i\text{-}Pr]_2$, together with a large number of titanium, zirconium, and cerium alkoxide compounds in solutions of boiling alcohol in an ebulliometer. In this way, the degree of polymerization, n, in metal oxo alkoxide compounds $[MO_x(OR)_{(y-2x)}]_n$ could be monitored as a function of the degree of hydrolysis, x, which was increased from a value of zero to a point where precipitation of insoluble products occurred. The absence of M–OH bonds could be established by elemental analysis and infrared spectroscopy. For the case of stannic isopropoxide $[Sn(O\text{-}i\text{-}Pr)_4 \cdot HO\text{-}i\text{-}Pr]_2$, which was observed to have a degree of oligomerization of 1.85 in boiling isopropanol, variation of the number average degree of oligomerization with the degree of hydrolysis (ratio of water molecules added per tin atom) revealed that the oxo-alkoxide oligomers conformed to a mixture of polymers $[Sn_2(\mu\text{-}O)_3(OR)_5]_n$ and $[Sn(\mu\text{-}O)_2(OR)_2]_n$ in the ratios 89.9 : 10.1%, respectively. Confirmation of the identity of such tin oxo-alkoxide polymers and determination of their structural preferences has yet to be investigated.

The further condensation of tin alkoxide compounds to form insoluble precipitates which yielded high purity SnO_2 upon sintering was patented by Thomas in 1976 [44]. Suwa et al. observed that hydrolysis of mixtures of titanium(IV) and tin(IV) alkoxide compounds in refluxing alcohols resulted in formation of particles with composition $Ti_{(1-x)}Sn_xO_2$. When the hydrolysis and subsequent thermal treatment was performed in the presence of a large excess of water (300 times the stoichiometric value), crystalline powders were obtained, while with a smaller water excess (70 times the stoichiometric value), amorphous metal oxides were formed. The crystalline products were found to be composed of particles with a crystallite size of 23–25 Å, which grew significantly upon heating to 630°C [76].

In other work, tin(IV) alkoxide compounds have been hydrolyzed under basic conditions analogous to those used by Stober et al. [77] to prepare silica spheres. Basic hydrolysis of the compounds $Sn(O\text{-}t\text{-}Bu)_4$, $[Sn(O\text{-}i\text{-}Pr)_4 \cdot HO\text{-}i\text{-}Pr]_2$ and $[Sn(OEt)_4]_n$ gave rise to the formation of sub-micron sized, crystalline, cassiterite particles [78,79]. Conditions were found under which monodispersed, spherical

particles with sizes in the region 70–250 nm could be prepared. An example of 250 nm spherical particles produced by this method is shown in Fig. 20.

TEM of the spherical particles shows that they are not homogeneous, but are made up of irregular grains of ~ 20–30 Å in diameter. Electron diffraction data from this material showed diffuse rings with d-spacings corresponding to the most intense reflections (110, 101 combined and 211, 220 combined) of SnO_2 (cassiterite). The grain size, measured by TEM, is consistent with the broadening of the X-ray powder diffraction lines for the spheres isolated *at the end* of the reaction, which correspond to approximately 20 Å-sized crystalline particles. Upon heating to 400°C, the X-ray powder pattern lines sharpen, consistent with SnO_2 (cassiterite), probably as a result of an increase in crystallite size. Recently, Ocana and Matijevic [80] have shown that spherical and rod-shaped tin oxide particles can be prepared by heating dilute solutions of tin(IV) chloride in the presence of urea or formamide.

The formation of dense, often spherical, metal oxide particles appears to be the thermodynamically preferred structure formed upon hydrolysis of metal alkoxide compounds under neutral pH or basic conditions. This probably results from the formation of oxo-alkoxide intermediates, such as those suggested by Bradley [81], where the coordination number of six is common and even eight is possible, in
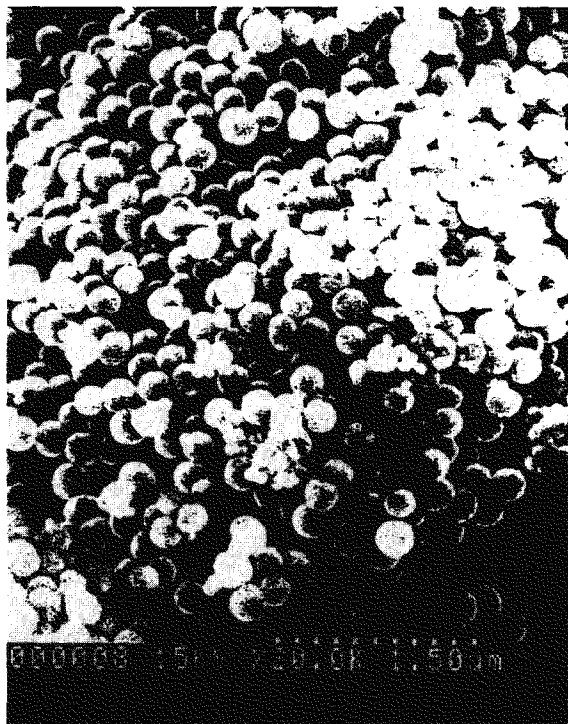

Fig. 20. SEM of 250 nm spherical particles produced by hydrolysis of $[Sn(OEt)_4]_n$.

contrast to the silicon system. However, dense powders are not necessarily desirable and often porous powders or films are more useful for various applications. Methods to achieve the greatest control over hydrolysis and condensation are currently being examined by a number of groups. Many different approaches are being explored, including the preparation of mixed ligand complexes and the addition of chelating agents to solutions of metal alkoxide compounds. At present, relatively little mechanistic data are available for either approach and no mechanistic data are available for tin(IV) alkoxide systems. However, there is a large body of patent literature in which processes for the formation of thin, dense, tin(IV) oxide films or porous powders have been identified. It has been suggested that the presence of alcoholamines or polyols during hydrolysis of tin(IV) alkoxide compounds or mixtures of metal alkoxide compounds suppresses hydrolysis [82]. Conductive indium tin oxide films with good adhesion and optical transparency (after firing) have been obtained from the hydrolysis of solutions of indium and tin alkoxide compounds containing any of the following reagents: monoethanolamine, diethanolamine, triethanolamine, mono-2-propanolamine, di-2-propanolamine, acetylacetone, ethylene glycol, diethylene glycol, propylene glycol, and dipropylene glycol [83]. Patterned metal oxide films have been obtained by dip-coating substrates in ethylene glycol containing metal alkoxide solutions, gelation of the film by hydrolysis, removal of selective areas of the film by wet etching and firing the remaining parts [84].

In one of the few studies of these systems, a solution containing tin tetraisopropoxide, triethanolamine, water, and isopropanol was prepared which exhibited a constant viscosity over 700 h [80]. Films formed from this solution (and from solutions to which [$Sb(OEt)_3$] had been added) after firing in air at 600°C for one hour, gave uniform dense thin films that were transparent in the visible region (95% undoped, 80% doped) and which had minimum resistivities of about 0.1 $\mu\Omega$ cm (undoped) and 0.005 Ω cm (doped) that were constant above film thicknesses of 2000 Å. Interestingly, it has been shown that resistivity varies as a function of film thickness in these systems and that precoating the glass substrate with 600 Å of TiO_2 reduced the resistivity of thin, tin oxide films. Preliminary results for a sol prepared from tin(IV) tertiary butoxide, ethanol, triethanolamine and water showed that the crystallinity of an underlying TiO_2 layer influenced the morphology of the cassiterite overlayer, presumably due to epitaxial relationships [85]. The films were composed of crystalline SnO_2 after firing to 600°C, as determined by X-ray powder diffraction. A number of processing parameters were studied, such as film thickness versus application number at different concentrations, which gave linear plots as expected for dip-coating processes. The morphology of the films was compared with that of tin(IV) oxide films deposited by CVD from $Sn(n\text{-}Bu)_4$ in O_2 [86]. The CVD films were found to have a rough, porous, island texture compared with the dip-coated films. The nature of the precursor solution was not investigated, and the presence of discrete molecular species or polymers is not known at this stage.

The preparation of porous metal oxide materials has been less extensively

investigated. Thin microporous layers have been obtained by acid-catalyzed condensation of metal alkoxide compounds followed by the addition of hydroxycellulose [87]. This solution was then applied to a porous silicon carbide support and fired at 700°C to give a metal oxide layer containing 100 Å pores with 40 vol.% porosity.

The formation of mixed metal oxides from mixed metal alkoxide compounds has recently received some attention as a method to control stoichiometry in these systems. For example, $LiNb(OEt)_6$ has been used as a molecular precursor for the formation of $LiNbO_3$ [88–90]. In the tin(IV) system, the compound $[ZnSn(OEt)_6]$ was studied as a model for ternary metal oxide systems [78]. Condensation of a benzene/THF/EtOH solution of $[ZnSn(OEt)_6]$ under basic conditions resulted in formation of crystalline *octahedral* particles of $[ZnSn(OH)_6]$, as shown in Fig. 21. In an analogous experiment, condensation of a THF solution of $[ZnSn(OEt)_6]$ resulted in the formation of large *spherical* particles of crystalline $[ZnSn(OH)_6]$, as shown in Fig. 22. Thermogravimetric analysis and differential scanning calorimetry of the spheres was consistent with endothermic loss of three equivalents of water by 200°C, to form an amorphous material at this temperature. Upon further heating, an exotherm was observed by differential scanning calorimetry at 676°C that corresponded to crystallization of $ZnSnO_3$ (ilmenite phase), analogous to the literature
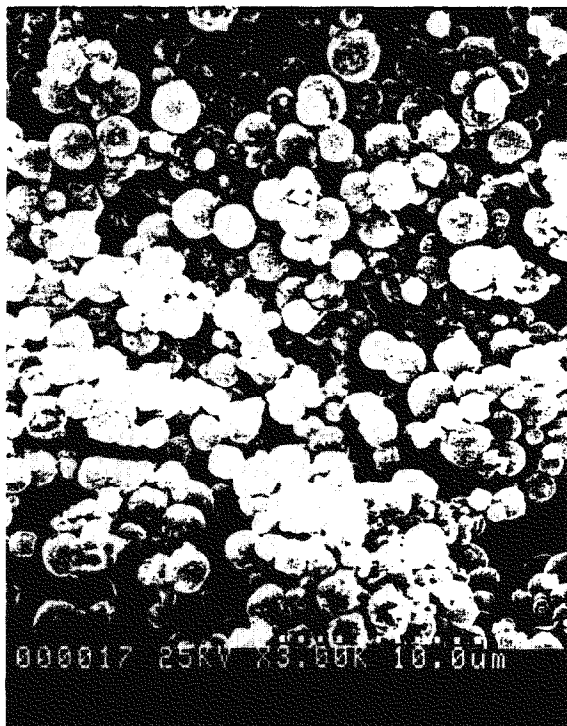

Fig. 21. SEM of crystalline spherical $[ZnSn(OH)_6]$ particles formed via basic hydrolysis of $[ZnSn(OEt)_6]$.

Fig. 22. SEM of crystalline octahedral [ZnSn(OH)$_6$] particles formed via basic hydrolysis of [ZnSn(OEt)$_6$].

data for [ZnSn(OH)$_6$]. Interestingly, when octahedral particles of [ZnSn(OH)$_6$] were heated, similar crystallization phenomena were observed and the octahedral habit of the particles was maintained, even at 1000°C. Close examination of the heated octahedral particles by SEM did not reveal any evidence of porosity within the resolution of this technique, in contrast to other crystalline metal hydroxide systems where increased porosity could be observed [91].

The mixed metal alkoxide compound [((1,5-COD)Rh)$_2$Sn(OEt)$_6$] has also been reacted with spherical, hydroxylated silica particles to produce a homogeneous dispersion of a species proposed to be siloxy-bound molecules according to the equation [92]

$$[((1,5COD)Rh)_2Sn(OEt)_6] + 2HO-Si\equiv$$

$$\rightarrow [((1,5\text{-}COD)Rh)_2Sn(OEt)_4(OSi\equiv)_2] + 2HOEt \qquad (23)$$
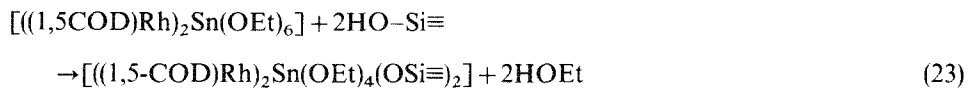
Upon thermal treatment under inert atmosphere or hydrogen, a dispersion of rhodium–tin alloy was formed on the silica surface, with a mean particle size of 24 Å. This system was found to be extremely active toward hydrogenation of ethylene and

benzene, while much less active toward hydrogenolysis of *n*-butane than silica-supported Rh catalysts prepared by traditional methods.

D. CONCLUSIONS

It appears that the structural variety observed for tin(IV) alkoxide compounds is similar to that observed for other electropositive metal alkoxide species. Studies to elucidate the solution structure of tin(IV) alkoxide compounds have the advantage, over many other metal alkoxide compounds, that the presence of NMR active isotopes may facilitate characterization. Hydrolysis of solutions containing tin(IV) alkoxide compounds have resulted in the formation of tin(IV) oxide powders and tin(IV) oxide films that are suitable for many applications. We anticipate that further studies in this area will lead to a more thorough understanding of the mechanistic aspects of "sol–gel"-type hydrolysis and condensation.

REFERENCES

1 D.C. Bradley, R.C. Mehrotra and D.P. Gaur, Metal Alkoxides, Academic Press, New York, 1978.
2 M.H. Chisholm and I.P. Rothwell, in G. Wilkinson, R.D. Gillard and J.A. McCleverty (Eds.), Comprehensive Coordination Chemistry, Pergamon Press, Oxford, 1987.
3 R.R. Schrock, Acc. Chem. Res., 24 (1990) 158.
4 S.S. Woodard, M.G. Finn and K.B. Sharpless, J. Am. Chem. Soc., 113 (1991) 106.
5 D.C. Bradley, Chem. Rev., 89 (1989) 1317.
6 L.G. Hubert-Pfaltzgraf, New J. Chem., 11 (1987) 663.
7 R.C. Mehrotra, in C.J. Brinker, D.E. Clark and D.R. Ulrich (Eds.), Better Ceramics Through Chemistry, Vol. III, Materials Research Society, Pittsburgh, 1988, p. 81.
8 R. Roy, Science, 238 (1987) 1664.
9 K.G. Caulton and L.G. Hubert-Pfalzgraf, Chem. Rev., 90 (1990) 969.
10 M.J. Hampden-Smith, D.S. Williams and A.L. Rheingold, Inorg. Chem., 29 (1990) 4067 and references cited therein.
11 J. Livage, M. Henry and C. Sanchez, Prog. Solid State Chem., 18 (1989) 259.
12 E.R. Myers and A. Kingon, Ferroelectric Thin Films, Mat. Res. Soc. Proc., 200 (1990).
13 M.S. Tomar and F.J. Garcia, Prog. Cryst. Growth Charact., 4 (1981) 221.
14 T.T. Kodas, Angew. Chem. Adv. Mater., 1 (1989) 189.
15 C.J. Brinker and G. Scherer, Sol–Gel Science, Academic Press, San Diego, 1990.
16 D.W. Schaeffer and K.D. Keefer, in L. Pietronero and E. Tosatti (Eds.), Fractals in Physics, North-Holland, Amsterdam, 1986, p. 39.
17 D.W. Schaeffer, Science, 243 (1989) 1023.

18 W.G. Klemperer and S.D. Ramamurthi, in C.J. Brinker, D.E. Clark and D.R. Ulrich (Eds.), Better Ceramics Through Chemistry, Vol. III, Materials Research Society, Pittsburgh, 1988, p. 1.

19 W.G. Klemperer, V.V. Mainz and D.M. Millar, in C.J. Brinker, D.E. Clark and D.R. Ulrich (Eds.), Better Ceramics Through Chemistry, Vol. II, Materials Research Society, Pittsburgh, 1986, pp. 3, 15.

20 J.A. Dean, Lange's Handbook of Chemistry, McGraw Hill, New York, 13th edn., 1985, Sect. 9.

21 R.C. Mehrotra, Adv. Inorg. Chem. Radiochem., 26 (1983) 269.

22 J.H. Jean and T.A. Ring, Langmuir, 2 (1986) 251.

23 E.A. Barringer and H.K. Bowen, Langmuir, 1 (1985) 414.

24 E.A. Barringer and H.K. Bowen, Langmuir, 1 (1985) 420.

25 E.A. Barringer and H.K. Bowen, J. Am. Ceram. Soc., 66 (1982) C-199.

26 B. Fegley and E.A. Barringer, in C.J. Brinker, D.E. Clark and D.R. Ulrich (Eds.), Better Ceramics Through Chemistry, Materials Research Society, Pittsburgh, 1984, p. 187.

27 S. Dick, C. Suhr, J.L. Rehspringer and M. Daire, Mater. Sci. Eng., A109 (1989) 227.

28 R.H. Heisland II, Y. Oguri, H. Okamura, W.C. Moffatt, B. Novich, E.A. Barringer and H.K. Bowen, in L.L. Hench and D.R. Ulrich (Eds.), Science of Ceramic Chemical Processing, Wiley, New York, 1986, p. 482.

29 E.A. Gulliver, T.A. Wark, J.W. Garvey, M.J. Hampden-Smith and A.K. Datye, J. Am. Cer. Soc., 74 (1991) 1091.

30 F. Babonneau, S. Doeuff, A. Leaustic, C. Sanchez, C. Cartier and M. Vergafuer, Inorg. Chem., 27 (1988) 3166.

31 C. Sanchez, F. Babonneau, S. Doeuff and A. Leaustic, in J.D. Mackenzie and D.R. Ulrich (Eds.), Ultrastructure Processing of Ceramics, Glasses and Composites, Wiley, New York, 1988.

32 S. Doeff, M. Henry, C. Sanchez and J. Livage, J. Non-Cryst. Solids, 89 (1987) 206.

33 C. Sanchez, J. Livage, M. Henry and F. Babonneau, J. Non-Cryst. Solids, 100 (1988) 65.

34 F. Babonneau, A. Leaustic and J. Livage, in C.J. Brinker, D.E. Clark and D.R. Ulrich (Eds.), Better Ceramics Through Chemistry, Vol. III, Materials Research Society, Pittsburgh, 1988, p. 317.

35 C. Sanchez, P. Toledano and F. Ribot, in C.J. Brinker, D.E. Clark and D.R. Ulrich (Eds.), Better Ceramics Through Chemistry, Vol. IV, Materials Research Society, Pittsburgh, 1990.

36 J. Livage, M. Henry, J.P. Jolivet and C. Sanchez, Mater. Res. Soc. Bull., 18 (1990).

37 D.C. Bradley, E.V. Caldwell and W. Wardlaw, J. Chem. Soc., (1957) 4775.

38 J.C. Marie, Ann. Chem., (1961) 969.

39 K.L. Chopra, S. Major and D.K. Pandya, Thin Solid Films, 102 (1983) 1.

40 G.D. Smith, P.E. Fanwick and I.P. Rothwell, J. Am. Chem. Soc., 111 (1989) 750.

41 G.D. Smith, P.E. Fanwick and I.P. Rothwell, Inorg. Chem., 29 (1990) 3221.

42 M.J. Hampden-Smith, T.A. Wark, A.L. Rheingold and J.C. Huffman, Can. J. Chem., 69 (1991) 121.

43 C.D. Chandler, G.D. Fallon, A.J. Koplick and B.O. West, Aust. J. Chem., 40 (1987) 1427.

44 I.M. Thomas, U.S. Pat. 3,946,056, 1974.

45 K. Jones and M.F. Lappert, J. Organomet. Chem., 295 (1965) 3.

46 I.P. Rothwell, personal communication, 1991.

47 M.H. Chisolm, D.L. Clark, K. Folting, J.C. Huffman and M.J. Hampden-Smith, J. Am. Chem. Soc., 109 (1987) 7700 and references cited therein.

48 D.C. Bradley, in W.L. Jolly (Ed.), Metal Alkoxides, Vol. 2, Interscience, New York, 1965.

49 R.C. Mehrotra and V.D. Gupta, J. Ind. Chem. Soc., 41 (1964) 537.

50 M. Vieth and M. Reimers, Chem. Ber., 123 (1990) 1941.

51 D.C. Bradley and H. Holloway, Can. J. Chem., 40 (1962) 1176.

52 M.J. Hampden-Smith, T.A. Wark and A.L. Rheingold, in preparation.

53 M.J. Hampden-Smith, T.A. Wark, E.A. Gulliver, L.C. Jones and J.W. Garvey, XXIV Organosilicon Symposium, El Paso, Texas, April 12th–13th, 1991.

54 T.A. Wark, E.A. Gulliver, M.J. Hampden-Smith and A.L. Rheingold, Inorg. Chem., 29 (1990) 4360.

55 M.J. Hampden-Smith, D.E. Smith and E.N. Duesler, Inorg. Chem., 27 (1989) 3399.

56 C. Chandler, G.D. Fallon and B.O. West, J. Chem. Soc. Chem. Commun., (1990) 1063.

57 J.D. Kennedy, W. McFarlane, P.J. Smith and R.F.M. White, J. Chem. Soc. Perkin Trans. 2, (1973) 1785.

58 R.K. Harris, Nuclear Magnetic Resonance Spectroscopy, Pitman, London, 1983.

59 R. Hani and R.A. Geanangel, Coord. Chem. Rev., 44 (1982) 229.

60 N.J. Clayden, C.M. Dobson and A. Fern, J. Chem. Soc. Dalton Trans., (1989) 843.

61 T.P. Lockhart, Inorg. Chem. 28 (1989) 4265.

62 T.P. Lockhart, H. Puff, W. Schuh, H. Reuter and T.N. Mitchell, J. Organomet. Chem., 366 (1989) 61.

63 M.J. Hampden-Smith, T.A. Wark and W. Earl, in preparation.

64 C.T. Lynch, K.S. Mazdiyazni, J.D. Smith and V.J. Crawford, Anal. Chem., 36 (1964) 2332.

65 D.P. Gaur, G. Srivastava and R.C. Mehrotra, J. Organomet. Chem., 221 (1973) 63.

66 J.A. Dean, Lange's Handbook of Chemistry, McGraw Hill, New York, 13th edn., 1985, Sect. 3–120.

67 R. Fiedler and H. Follner, Monatsh. Chem., 108 (1977) 319.

68 H. Follner, Monatsh. Chem., 103 (1972) 1438.

69 S.C. Goel, M.Y. Chiang and W.E. Buhro, Inorg. Chem., 29 (1990) 4640.

70 T.A. Wark, E.A. Gulliver, L.C. Jones, M.J. Hampden-Smith, A.L. Rheingold and J.C. Huffman, in C.J. Brinker, D.E. Clark and D.R. Ulrich (Eds.), Better Ceramics Through Chemistry, Vol. IV, Materials Research Society, Pittsburgh, 1990, p. 61.

71 M.J. Hampden-Smith and T.A. Wark, unpublished results.

72 M. Veith and R. Rosler, Angew. Chem. Int. Ed. Engl., 21 (1982) 558.

73 R. Rosler and M. Veith, Z. Naturforsch. Teil B, 41 (1986) 1071.

74 M. Vieth, D. Kafer and V. Huch, Angew. Chem., 25 (1986) 375.

75 R.C. Mehrotra, A.K. Roi and N.C. Jain, J. Inorg. Nucl. Chem., 40 (1978) 349.

76 Y. Suwa, Y. Kato, S. Hirano and S. Naka, Zairyo, 31 (1982) 955.

77 W. Stober, A. Fink and E. Bohn, J. Colloid Interface Sci., 81 (1981) 354.

78 E.A. Gulliver, J.W. Garvey, T.A. Wark, M.J. Hampden-Smith and A.K. Datye, J. Am. Ceram. Soc., 74 (1991) 1091.

79 E.A. Gulliver, J.W. Garvey, T.A. Wark, M.J. Hampden-Smith and A.K. Datye, Mat. Res. Soc. Symp. Proc., Symp. S, Fall Meeting, Boston, 1990.

80 M. Ocana and E. Matijevic, J. Mater. Res., 5 (1990) 1083.

81 D.C. Bradley, Coord. Chem. Rev., 2 (1967) 299.

82 Y. Takahashi and Y. Wada, J. Electrochem. Soc., 137 (1990) 267.

83 T. Suzuki, M. Matsuki and K. Kobayaski, Kokai Tokkyo Koho, (1989) 76; Chem. Abstr., 112 (26) (1990) 244292u.

84 K. Makita, A. Hattori and K. Tanaka, Ger. Offen. 57–60 (1989); Chem. Abstr. 111(16) (1989) 139322k.

85 M.J. Hampden-Smith, C.J. Brinker and I.A. Weinstock, in preparation.

86 Y. Takahashi and Y. Wada, Yogyo Kyokai Shi, (1987) 57; Chem. Abstr., 107(18) (1987) 159985z.

87 J. Herzig, A. Nudelman and H.E. Gottlieb, Carbohydr. Res., 117 (1988) 21.

88 D.J. Eichorst, D.A. Payne, S.R. Wilson and K.E. Howard, Inorg. Chem., 29 (1990) 1459.

89 L.F. Francis, D.A. Payne and S.R. Wilson, Chem. Mater., 2 (1990) 645.

90 J. Campion and D.A. Payne, Mater. Res. Soc. Symp. Proc., Fall Meeting, Boston, 1990, Abstr. E6–12.

91 M. Inagaki, T. Kuroishi, Y. Yomashita and M. Urata, Z. Anorg. Allgem. Chem., 527 (1985) 193.

92 S.L. Anderson, A.K. Datye, T.A. Wark and M.J. Hampden-Smith, Catal. Lett., 8 (1991) 345.